Physica D 427 (2021) 133020

Contents lists available at ScienceDirect

Physica D

journal homepage: www.elsevier.com/locate/physd

Instability theory of kink and anti-kink profiles for the sine–Gordon equation on Josephson tricrystal boundaries

Jaime Angulo Pava [a,*], Ramón G. Plaza [b]

[a] Department of Mathematics, IME-USP, Rua do Matão 1010, Cidade Universitária, CEP 05508-090, São Paulo, SP, Brazil
[b] Instituto de Investigaciones en Matemáticas Aplicadas y en Sistemas, Universidad Nacional Autónoma de México, Circuito Escolar s/n, Ciudad Universitaria, C.P. 04510 Cd. de México, Mexico

ARTICLE INFO

Article history:
Received 9 April 2021
Received in revised form 17 July 2021
Accepted 20 August 2021
Available online 30 August 2021
Communicated by P. Kevrekidis

Keywords:
sine–Gordon model
Josephson tricrystal junction
Kink
Anti-kink solitons
Extension theory
Instability

ABSTRACT

The aim of this work is to establish an instability study for stationary kink and antikink/kink profiles solutions for the sine–Gordon equation on a metric graph with a structure represented by a $\mathcal{Y}$-junction so-called a Josephson tricrystal junction. By considering boundary conditions at the graph-vertex of δ'-interaction type, it is shown that kink profiles which are continuous at the vertex, as well as anti-kink/kink profiles possibly discontinuous at the vertex, are linearly (and nonlinearly) unstable. The extension theory of symmetric operators, Sturm–Liouville oscillation results and analytic perturbation theory of operators are fundamental ingredients in the stability analysis. The local well-posedness of the sine–Gordon model in $H^1(\mathcal{Y})\times L^2(\mathcal{Y})$ is also established. The theory developed in this investigation has prospects for the study of the (in)-stability of stationary wave solutions of other configurations for kink-solitons profiles.

1. Introduction

Nonlinear dispersive models on quantum star-shaped graphs (quantum graphs, henceforth) arise as simplifications for wave propagation, for instance, in quasi one-dimensional (e.g. meso- or nano-scaled) systems that *look like a thin neighborhood of a graph*. We recall that a star-shaped metric graph, $\mathcal{G}$, is a structure represented by a finite or countable edges attached to a common vertex, $\nu = 0$, having each edge identified with a copy of the half-line, $(-\infty, 0)$ or $(0, \infty)$ (see Fig. 1). Hence, a quantum star-shaped metric graph, $\mathcal{G}$, is a star-shaped metric graph with a linear Hamiltonian operator (for example, a Schrödinger-like operator) suitably defined on functions which are supported on the edges.

Quantum graphs have been used to describe a variety of physical problems and applications, for instance, condensed matter, $\mathcal{Y}$-Josephson junction networks, polymers, optics, neuroscience, DNA chains, blood pressure waves in large arteries, or in shallow water models describing a fluid networks (see [1–5] and the many references therein). Recently, they have attracted much attention in the context of soliton transport in networks and branched structures since wave dynamics in networks can be modeled by nonlinear evolution equations (see, e.g., [6–14]).

The present study focuses on the dynamics of the one-dimensional sine–Gordon equation,

$$u_{tt} - c^2 u_{xx} + \sin u = 0, \tag{1.1}$$

posed on a metric graph. The sine–Gordon model appears in a great variety of physical and biological models. For example, it has been used to describe the magnetic flux in a long Josephson line in superconductor theory [15–17], mechanical oscillations of a nonlinear pendulum [18,19] and the dynamics of a crystal lattice near a dislocation [20]. Recently, soliton solutions to Eq. (1.1) have been used as simplified models of scalar gravitational fields in general relativity theory [21,22] and of oscillations describing the dynamics of DNA chains [23,24] in the context of the *solitons in DNA hypothesis* [25]. In addition, the sine–Gordon equation (1.1) underlies many remarkable mathematical features such as a Hamiltonian structure [26], complete integrability [27,28] and the existence of localized solutions (solitons) [29,30].

In recent contributions (cf. [10,11]), we performed the first rigorous analytical studies of the stability properties of stationary soliton solutions of kink and/or anti-kink profiles to the sine–Gordon equation *posed on a $\mathcal{Y}$-junction graph*. There exist two main types of $\mathcal{Y}$-junctions. A $\mathcal{Y}$-junction of the first type (or type I) consists of one incoming (or parent) edge, $E_1 = (-\infty, 0)$, meeting at one single vertex at the origin, $\nu = 0$, with other two outgoing (children) edges, $E_j = (0, \infty)$, $j = 2, 3$. The second type (or $\mathcal{Y}$-junction of type II) resembles more a starred structure and consists of three identical edges of the form $E_j = (0, \infty)$,

* Corresponding author.
E-mail addresses: angulo@ime.usp.br (J.A. Pava), plaza@mym.iimas.unam.mx (R.G. Plaza).

https://doi.org/10.1016/j.physd.2021.133020

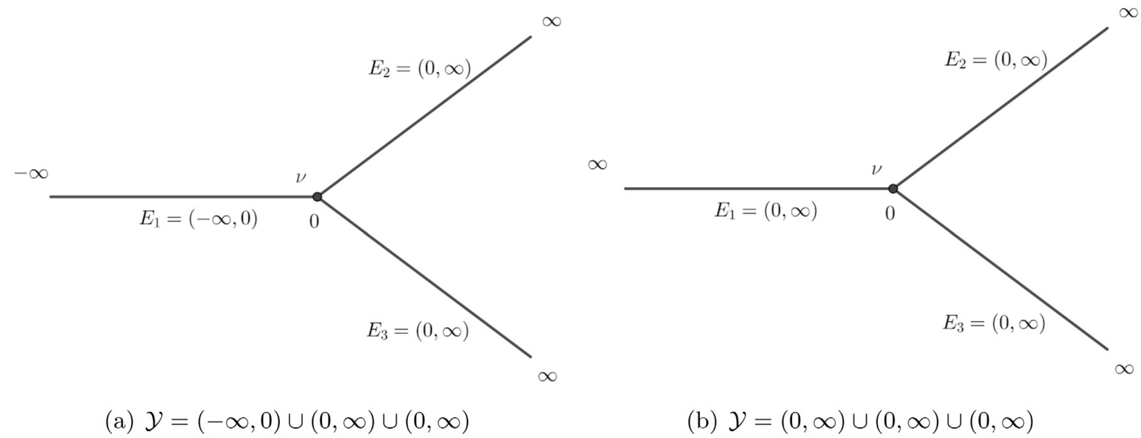

Fig. 1. Panel (a) shows a $\mathcal{Y}$-junction of the first type with $E_1 = (-\infty, 0)$ and $E_j = (0, \infty)$, $j = 2, 3$, whereas panel (b) shows a $\mathcal{Y}$-junction of the second type (star graph) with $E_j = (0, \infty)$, $1 \leqq j \leqq 3$.

$1 \leqq j \leqq 3$. See Fig. 1(b) for an illustration. Junctions of type I are more common in unidirectional fluid flow models (see, for example, [31]). The junctions of the second type (which belong to the star graph class) are often referred as *Josephson tricrystal junctions* and are common in network of transmission lines (see, for instance, [13,32,33]). The distinction between the two types of $\mathcal{Y}$-junctions is mainly historical.

Our work focuses on the sine–Gordon model posed on a $\mathcal{Y}$-tricrystal junction, more precisely, on the equations

$$\partial_t^2 u_j - c_j^2 \partial_x^2 u_j + \sin u_j = 0, \qquad x \in E_j = (0, \infty), \ \ t > 0, \ \ 1 \leqq j \leqq 3, \tag{1.2}$$

where $u_j = u_j(x, t)$. It is assumed that the characteristic speed on each edge E_j is constant and positive, $c_j > 0$, without loss of generality.

Posing the sine–Gordon equation on a metric graph comes out naturally from practical applications. Indeed, in the context of superconductor theory, the sine–Gordon equation on a metric graph arises as a model for coupling of two or more Josephson junctions in a network. A Josephson junction is a quantum mechanical structure that is made by two superconducting electrodes separated by a barrier (the junction), thin enough to allow coupling of the wave functions of electrons for the two superconductors [34]. After appropriate normalizations, it can be shown that the phase difference u (also known as order parameter) of the two wave functions satisfies the sine–Gordon equation (1.1) [15,34]. Coupling three junctions at one common vertex, the so called tricrystal junction, can be regarded (and fabricated) as a probe of the order parameter symmetry of high temperature superconductors (cf. [35,36]). Physically coupling three otherwise independent long Josephson junctions, $\mathcal{Y} = \cup_{j=1}^3 E_j$, together at one common vertex, was first proposed by Nakajima et al. [37,38] as a prototype for logic circuits.

What is more crucial in the analysis on quantum graphs is the choice of boundary conditions, mainly because the transition rules at the vertex completely determine the dynamics of the PDE model on the graph. For the sine–Gordon equation in $\mathcal{Y}$-junctions, previous studies have basically (and almost exclusively) considered two types of boundary conditions: interactions of δ -type (continuity of the wave functions plus a law of Kirchhoff-type for the fluxes at the vertex, see [3,10,39]) and of δ'-type (continuity of the derivatives plus a Kirchhoff law for the self-induced magnetic flux). Since Josephson models arise in the description of electromagnetic flux, interactions of δ'-type have received more attention (see, for example, [11,13,32,37,38,40]). Thus, since the surface current density should be the same in all three films at the vertex, Nakajima et al. [37,38] (see also [32,40]) impose the condition

$$c_1 \partial_x u_{1\,|x=0} = c_2 \partial_x u_{2\,|x=0} = c_3 \partial_x u_{3\,|x=0}, \tag{1.3}$$

expressing that the magnetic field, which is proportional to the derivative of phase difference, should be continuous at the intersection. Moreover, the magnetic flux computed along an infinitesimal small contour encircling the origin (vertex) must vanish, that is, the total change of the gauge invariant phase difference must be zero [14,32]. This leads to the Kirchhoff-type of boundary condition

$$\sum_{j=1}^{3} c_j u_j(0+) = 0. \tag{1.4}$$

The interaction conditions (1.3)–(1.4) are known as boundary conditions of δ'-type: they express continuity of the fluxes (derivatives) plus a Kirchhoff-type rule for the self-induced magnetic flux.

Motivated by physical applications, the purpose of the present paper is to study the stability of particular stationary solutions to the sine–Gordon equation seen as a first order system posed on a $\mathcal{Y}$-tricrystal junction, namely, the system

$$\begin{cases} \partial_t u_j = v_j \\ \partial_t v_j = c_j^2 \partial_x^2 u_j - \sin u_j, \end{cases} \qquad x \in E_j = (0, \infty), \ \ t > 0, \ \ 1 \leqq j \leqq 3. \tag{1.5}$$

As far as we know, there is no rigorous analytical study of the stability of stationary solutions of type kink and/or anti-kink to the vectorial sine–Gordon model (1.5) on a tricrystal junction with boundary conditions of δ'-interaction type available in the literature (see Angulo and Plaza [11] for related results). The stability of these static configurations is an important property from both the mathematical and the physical points of view. Stability can predict whether a particular state can be observed in experiments or not. Unstable configurations are rapidly dominated by dispersion, drift, or by other interactions depending on the dynamics, and they are practically undetectable in applications.

For tricrystal junctions we will study stationary solutions with a kink type structure. The latter have the form $u_j(x, t) = \varphi_j(x)$, $v_j(x, t) = 0$, for all $j = 1, 2, 3$, and $x \in E_j$, $t > 0$, in (1.5), where each of the profile functions φ_j satisfies the equation

$$-c_j^2 \varphi_j'' + \sin \varphi_j = 0, \tag{1.6}$$

on each edge $E_j = (0,\infty)$ and for all j, as well as the boundary conditions of δ'-type, at the vertex $\nu = 0$:

$$c_1\varphi_1'(0+) = c_2\varphi_2'(0+) = c_3\varphi_3'(0+), \quad \sum_{j=1}^{3} c_j\varphi_j(0+) = \gamma c_1\varphi_1'(0+). \tag{1.7}$$

These conditions depend upon the real parameter γ, whose range will depend of the specific profile (φ_j) to be found. Therefore, the value $\gamma\in\mathbb{R}$ is part of the physical parameters that determine the model (such as the speeds c_j, for instance). Instead of adopting *ad hoc* boundary conditions, we consider a parametrized family of transition rules covering a wide range of applications and which, for the particular value $\gamma = 0$, include the Kirchhoff condition (1.4) previously studied in the literature. Our analysis focuses on two particular class of solutions of the sine–Gordon equation known as *kink* and *anti-kink* (also referred to as topological solitons) [18,29,30].

Initially, we look at the particular family of solutions with the same kink-type structure with $c_j > 0$,

$$\varphi_j(x) = 4\arctan\left(e^{-(x-b_j)/c_j}\right), \qquad x\in(0,\infty),\ \ j=1,2,3, \tag{1.8}$$

where the constants b_j are determined by the boundary conditions (1.7). The family satisfies as well

$$\varphi_j(+\infty) = 0, \qquad j=1,2,3, \tag{1.9}$$

and $\Phi = (\varphi_j)_{j=1}^3 \in H^2(\mathcal{Y})$ (see definition of the Sobolev space $H^2(\mathcal{Y})$ on a $\mathcal{Y}$-junction graph in the Notation section below). Our second class of solutions are the anti-kink/kink type soliton, namely, profiles having the form

$$\begin{cases} \varphi_1(x) = 4\arctan\left(e^{(x-a_1)/c_1}\right), & x\in(0,\infty), \\ \quad \lim_{x\to+\infty}\varphi_1(x) = 2\pi, & \\ \varphi_j(x) = 4\arctan\left(e^{(x-a_j)/c_j}\right) - 2\pi, & x\in(0,\infty), \\ \quad \lim_{x\to+\infty}\varphi_j(x) = 0 \ \ j=2,3, & \end{cases} \tag{1.10}$$

where each a_j is a constant determined by the boundary conditions (1.7). Expression in (1.10) is so-called 2π-kink because the total Josephson phase is 2π when one circles the branch point at large distances, i.e., $\sum_{j=1}^3 \varphi_j(+\infty) = 2\pi$. We have left open the stability study of other Josephson configurations systems, such as a tricrystal junction with a π-kink, $\phi_1(x) = 4\arctan\left(e^{(x-a_1)/c_1}\right) - \pi$, $\phi_j(x) = 4\arctan\left(e^{(x-a_j)/c_j}\right) - 2\pi$, $j = 2,3$. This stability analysis is also important for experimentalists since these network systems constitute a large opportunity for applications in high-performance computers (see [13] and references therein).

In the forthcoming analysis we establish the existence of two smooth mapping of stationary profiles for (1.5), the first one $\lambda\in(-\infty,-\sum_{j=1}^3 c_j) \to \Pi_{\lambda,\delta'} := (\varphi_1,\varphi_2,\varphi_3,0,0,0)\in H^2(\mathcal{Y})\times L^2(\mathcal{Y})$, with $\varphi_j = \varphi_{j,b_j(\lambda)}$ defined in (1.8), and the second one $Z\in(-\infty,\infty)\to \Phi_{Z,\delta'} := (\varphi_1,\varphi_2,\varphi_3,0,0,0)\in \mathcal{Z}(\mathcal{Y})\times L^2(\mathcal{Y})$, with $\varphi_j = \varphi_{j,a_j(Z)}$ defined in (1.10), and both families satisfying the δ'-type interaction condition in (1.7). Here, we have used the notation $\mathcal{Z}(\mathcal{Y}) := H^2_{loc}(-\infty,0)\times H^2(0,\infty)\times H^2(0,\infty)$.

The main linear instability results of this manuscript are the following,

Theorem 1.1. *Let $\lambda\in(-\infty,-\sum_{j=1}^3 c_j)$ and consider the smooth family of stationary profiles $\lambda\mapsto\Pi_{\lambda,\delta'}$, which, in addition, satisfy the continuity condition at the vertex, more precisely, $\varphi_1(0+) = \varphi_2(0+) = \varphi_3(0+)$. Then $\Pi_{\lambda,\delta'}$ is linear and nonlinearly unstable for the sine–Gordon model (2.1) on a tricrystal junction in the following cases:*

(1) for $\lambda\in(-\frac{\pi}{2}\sum_{j=1}^3 c_j, -\sum_{j=1}^3 c_j)$ and $c_i > 0$,

(2) for $\lambda\in(-\infty,-\frac{\pi}{2}\sum_{j=1}^3 c_j]$ and $c_1 = c_2 = c_3$.

Theorem 1.2. *Let $c_1 = c_2 = c_3$, $Z\in(-\infty,+\infty)$, and the smooth family of stationary anti-kink/kink profiles $Z\to\Phi_{Z,\delta'}$ determined above. Then $\Phi_{Z,\delta'}$ is spectrally unstable for the sine–Gordon model (1.5) on a tricrystal junction.*

We refer the reader to Remarks 3.6 and 3.12 for comments on the cases where the constants c_j are not all equal in the Theorems above.

In our stability analysis below, the family of linearized operators around the stationary profiles plays a fundamental role. These operators are characterized by the following formal Schrödinger diagonal matrix operators,

$$\mathcal{W}\mathbf{v} = \left(\left(-c_j^2\frac{d^2}{dx^2}v_j + \cos(\varphi_j)v_j\right)\delta_{j,k}\right), \quad 1 \leqq j,k \leqq 3, \quad \mathbf{v} = (v_j)_{j=1}^3, \tag{1.11}$$

(where $\delta_{j,k}$ denotes the Kronecker symbol), and which become self-adjoint operators on domains with δ'-type interaction at the vertex $\nu = 0$,

$$D(\mathcal{W}) = \left\{ \mathbf{v} = (v_j)_{j=1}^3 \in H^2(\mathcal{Y}) : c_1v_1'(0+) = c_2v_2'(0+) = c_3v_3'(0+), \ \sum_{j=1}^3 c_jv_j(0+) = \gamma c_1v_1'(0+) \right\}, \tag{1.12}$$

with $\gamma\in\mathbb{R}$. It is to be observed that the particular family (1.8) of kink-profile stationary solutions under consideration is such that $(\varphi_j)_{j=1}^3\in D(\mathcal{W})$ in view that they satisfy the boundary conditions (1.7) with $\gamma\equiv\lambda\in(-\infty,-\frac{\pi}{2}\sum_{j=1}^3 c_j]$.

In Section 2 we establish a general instability criterion for static solutions for the sine–Gordon model (1.5) on a $\mathcal{Y}$-junction. The reader can find this result in Theorem 2.4. It essentially provides sufficient conditions on the flow of the semigroup generated by the linearization around the stationary solutions (see (2.7)), for the existence of a pair of positive/negative real eigenvalues of this linearization, which depend of the Morse index for the associated self-adjoint operator $(\mathcal{W}, D(\mathcal{W}))$ (see assumptions (S_1)–(S_2)–(S_3) in the end of Section 2). The proof of Theorems 1.1 and 1.2 follow as an application of Theorem 2.4. It is to be observed that this instability criterion is very versatile, as it can be applied to different interactions at the vertex, such as the δ-type (see [10]). Moreover, we believe that for other metric graph configurations for the sine–Gordon model, such as tree graphs (see [33]), our instability criterion can be a useful tool in the study of stability properties of stationary profiles.

The structure of the paper is the following: in Section 2, we review the general instability criterion for stationary solutions for the sine–Gordon model (1.5) on a $\mathcal{Y}$-junction developed in [10] (see Theorem 2.4; see also [41]). The Section 3.1 is devoted to develop the instability theory of kink-profiles and we show Theorem 1.1. A special space is defined in order to analyze the Cauchy problem in $H^1(\mathcal{Y})\times L^2(\mathcal{Y})$. Section 3.2 is devoted to the proof of Theorem 1.2. By convenience of the reader and by the sake of completeness we establish in the Appendix some results of the extension theory of symmetric operators used in the body of the manuscript.

On notation

For any $-\infty\le a<b\le\infty$, we denote by $L^2(a,b)$ the Hilbert space equipped with the inner product $(u,v) = \int_a^b u(x)\overline{v(x)}dx$. By $H^n(a,b)$ we denote the classical Sobolev spaces on $(a,b)\subseteq\mathbb{R}$ with the usual norm. We denote by $\mathcal{Y}$ the junction of type II

parametrized by the edges $E_j = (0, \infty)$, $j = 1, 2, 3$, attached to a common vertex $\nu = 0$. On the graph $\mathcal{Y}$ we define the classical L^p-spaces

$$L^p(\mathcal{Y}) = L^p(0, +\infty) \oplus L^p(0, +\infty) \oplus L^p(0, +\infty), \quad p > 1,$$

and Sobolev-spaces $H^m(\mathcal{Y}) = H^m(0, +\infty) \oplus H^m(0, +\infty) \oplus H^m(0, +\infty)$, $m \in \mathbb{N}$, with the natural norms. Also, for $\mathbf{u} = (u_j)_{j=1}^3$, $\mathbf{v} = (v_j)_{j=1}^3 \in L^2(\mathcal{Y})$, the inner product is defined by

$$\langle \mathbf{u}, \mathbf{v} \rangle = \sum_{j=1}^{3} \int_0^\infty u_j(x)\overline{v_j(x)}\, dx$$

Depending on the context we will use the following notations for different objects. By $\|\cdot\|$ we denote the norm in $L^2(\mathbb{R})$ or in $L^2(\mathcal{Y})$. By $\|\cdot\|_p$ we denote the norm in $L^p(\mathbb{R})$ or in $L^p(\mathcal{Y})$. Finally, if A is a closed, densely defined symmetric operator in a Hilbert space H then its domain is denoted by $D(A)$, the deficiency indices of A are denoted by $n_\pm(A) := \dim\ker(A^* \mp iI)$, where A^* is the adjoint operator of A, and the number of negative eigenvalues counting multiplicities (or Morse index) of A is denoted by $n(A)$.

2. Preliminaries: Linear instability criterion for sine–Gordon model on a tricrystal junction

We start our study by recasting the equations in (1.5) in the vectorial form

$$\mathbf{w}_t = JE\mathbf{w} + F(\mathbf{w}) \tag{2.1}$$

where $\mathbf{w} = (u, v)^\top$, with $u = (u_1, u_2, u_3)^\top$, $v = (v_1, v_2, v_3)^\top$, $u_j, v_j : E_j \to \mathbb{R}$, $1 \leqq j \leqq 3$,

$$J = \begin{pmatrix} 0 & I_3 \\ -I_3 & 0 \end{pmatrix}, \quad E = \begin{pmatrix} \mathcal{T} & 0 \\ 0 & I_3 \end{pmatrix},$$

$$F(\mathbf{w}) = \begin{pmatrix} 0 \\ 0 \\ 0 \\ -\sin(u_1) \\ -\sin(u_2) \\ -\sin(u_3) \end{pmatrix}, \tag{2.2}$$

and where I_3 denotes the identity matrix of order 3 and $\mathcal{T}$ is the diagonal-matrix linear operator

$$\mathcal{T} = \left(\left(-c_j^2 \frac{d^2}{dx^2}\right)\delta_{j,k}\right), \quad 1 \leqq j, k \leqq 3. \tag{2.3}$$

For the $\mathcal{Y}$-junction being a tricrystal junction, we will use the δ'-interaction domain for $\mathcal{T}_\gamma \equiv \mathcal{T}$ given by (1.12), namely, $D(\mathcal{T}_\gamma) = D(\mathcal{W})$:

$$D(\mathcal{T}_\gamma) := \{(v_j)_{j=1}^3 \in H^2(\mathcal{Y}) : c_1 v_1'(0+) = c_2 v_2'(0+) = c_3 v_3'(0+), \\ \sum_{j=1}^{3} c_j v_j(0+) = \gamma c_1 v_1'(0+)\}, \tag{2.4}$$

with $\gamma \in \mathbb{R}$ (see Proposition 3.1).

In the sequel, we review the linear instability criterion developed in [10] (see also [41]). Although the stability analysis in [10] pertains to interactions of δ-type at the vertex, it is important to note that the criterion proved in that references also applies to any type of stationary solutions independently of the boundary conditions under consideration and, therefore, it can be used to study the present configurations with boundary rules at the vertex of δ'-interaction type, or even to other types of stationary solutions to the sine–Gordon equation such as anti-kinks, for instance. In addition, the criterion applies to both the $\mathcal{Y}$-junction of type I (see Fig. 1) and of type II (see Fig. 1(b)).

Let $\mathcal{Y}$ be a tricrystal junction. Let us suppose that JE on a domain denoted as $D(JE) \subset H^1(\mathcal{Y}) \times L^2(\mathcal{Y})$ is the infinitesimal generator of a C_0-semigroup on $H^1(\mathcal{Y}) \times L^2(\mathcal{Y})$ and that there exists a stationary solution $\Upsilon = (\zeta_1, \zeta_2, \zeta_3, 0, 0, 0) \in D(JE)$. Thus, every component ζ_j satisfies the equation

$$-c_j^2 \zeta_j'' + \sin(\zeta_j) = 0, \quad j = 1, 2, 3. \tag{2.5}$$

Now, we suppose that $\mathbf{w}$ satisfies formally equality in (2.1) and we define

$$\mathbf{v} \equiv \mathbf{w} - \Upsilon, \tag{2.6}$$

then, from (2.5) we obtain the following linearized system for (2.1) around $\Phi = (\zeta_j)_{j=1}^3$,

$$\mathbf{v}_t = J\mathcal{E}\mathbf{v}, \tag{2.7}$$

with $\mathcal{E}$ being the 6×6 diagonal-matrix $\mathcal{E} = \begin{pmatrix} \mathcal{L} & 0 \\ 0 & I_3 \end{pmatrix}$, and

$$\mathcal{L} = \left(\left(-c_j^2 \frac{d^2}{dx^2} + \cos(\zeta_j)\right)\delta_{j,k}\right), \quad 1 \leqq j, k \leqq 3. \tag{2.8}$$

We point out the equality $J\mathcal{E} = JE + \mathcal{Z}$, with

$$\mathcal{Z} = \begin{pmatrix} 0 & 0 \\ (-\cos(\zeta_j)\delta_{j,k}) & 0 \end{pmatrix} \tag{2.9}$$

being a *bounded* operator on $H^1(\mathcal{Y}) \times L^2(\mathcal{Y})$. This implies that $J\mathcal{E}$ also generates a C_0-semigroup on $H^1(\mathcal{Y}) \times L^2(\mathcal{Y})$ (see Pazy [42]).

The linear instability criterion below provides sufficient conditions for the trivial solution $\mathbf{v} \equiv 0$ to be unstable by the linear flow of (2.7). More precisely, it underlies the existence of a *growing mode solution* to (2.7) of the form $\mathbf{v} = e^{\mu t}\Psi$ and $\mathrm{Re}\,\mu > 0$. To find it, one needs to solve the formal system

$$J\mathcal{E}\Psi = \mu\Psi, \tag{2.10}$$

with $\Psi \in D(J\mathcal{E})$. If we denote by $\sigma(J\mathcal{E}) = \sigma_{\mathrm{pt}}(J\mathcal{E}) \cup \sigma_{\mathrm{ess}}(J\mathcal{E})$ the spectrum of $J\mathcal{E}$ (namely, $\mu \in \sigma_{\mathrm{pt}}(J\mathcal{E})$ if μ is isolated and with finite multiplicity) then we have the following

Definition 2.1. The stationary vector solution $\Upsilon \in D(\mathcal{E})$ is said to be *spectrally stable* for model sine–Gordon (2.1) if the spectrum of $J\mathcal{E}$, $\sigma(J\mathcal{E})$, satisfies $\sigma(J\mathcal{E}) \subset i\mathbb{R}$. Otherwise, the stationary solution $\Upsilon \in D(\mathcal{E})$ is said to be *spectrally unstable*.

Remark 2.2. It is well-known that $\sigma_{\mathrm{pt}}(J\mathcal{E})$ is symmetric with respect to both the real and imaginary axes and $\sigma_{\mathrm{ess}}(J\mathcal{E}) \subset i\mathbb{R}$ under the assumption that J is skew-symmetric and that $\mathcal{E}$ is self-adjoint (by supposing, for instance, Assumption (S_3) below for $\mathcal{L}$; see [43, Lemma 5.6 and Theorem 5.8]). These cases on J and $\mathcal{E}$ are considered in the theory. Hence, it is equivalent to say that $\Upsilon \in D(\mathcal{E})$ is *spectrally stable* if $\sigma_{\mathrm{pt}}(J\mathcal{E}) \subset i\mathbb{R}$, and it is spectrally unstable if $\sigma_{\mathrm{pt}}(J\mathcal{E})$ contains a point μ with $\mathrm{Re}\,\mu > 0$.

It is widely known that the spectral instability of a specific traveling wave solution of an evolution type model is a key prerequisite to show their nonlinear instability property (see [43–45] and the references therein). Thus we have the following definition.

Definition 2.3. The stationary vector solution $\Upsilon \in D(\mathcal{E})$ is said to be *nonlinearly unstable* in $X \equiv H^1(\mathcal{Y}) \times L^2(\mathcal{Y})$-norm for model sine–Gordon (2.1) if there is $\epsilon > 0$ such that for every $\delta > 0$ there exist an initial data $\mathbf{w}_0$ with $\|\Upsilon - \mathbf{w}_0\|_X < \delta$ and an instant $t_0 = t_0(\mathbf{w}_0)$, such that $\|\mathbf{w}(t_0) - \Upsilon\|_X > \epsilon$, where $\mathbf{w} = \mathbf{w}(t)$ is the solution of the sine–Gordon model with initial data $\mathbf{w}(0) = \mathbf{w}_0$.

From (2.10), the eigenvalue problem to solve is now reduced to the abstract problem

$$J\mathcal{E}\Psi = \mu\Psi, \quad \mathrm{Re}\,\mu > 0, \quad \Psi \in D(\mathcal{E}). \tag{2.11}$$

Next, we establish our theoretical framework and assumptions for obtaining a nontrivial solution to problem in (2.11):

- (S_1) $J\mathcal{E}$ is the generator of a C_0-semigroup $\{S(t)\}_{t\geqq 0}$.
- (S_2) Let $\mathcal{L}$ be the matrix-operator in (2.8) defined on a domain $D(\mathcal{L}) \subset L^2(\mathcal{Y})$ on which $\mathcal{L}$ is self-adjoint.
- (S_3) Suppose $\mathcal{L} : D(\mathcal{L}) \to L^2(\mathcal{Y})$ is invertible with Morse index $n(\mathcal{L}) = 1$ and such that $\sigma(\mathcal{L}) = \{\lambda_0\} \cup J_0$ with $J_0 \subset [r_0, +\infty)$, for $r_0 > 0$, and $\lambda_0 < 0$,

The criterion for linear instability of the trivial solution $\mathbf{v} \equiv 0$ of (2.7) reads precisely as follows (cf. [10]).

Theorem 2.4 (*Linear Instability Criterion*)**.** *Suppose the assumptions (S_1) - (S_3) hold. Then the operator $J\mathcal{E}$ has a real positive and a real negative eigenvalue.*

Proof. See [10,41]. □

3. Instability of stationary solutions for the sine–Gordon equation with δ'-interaction on a tricrystal junction

In this section we study the stability of stationary solutions determined by a δ'-interaction type at the vertex $\nu = 0$ of a tricrystal junction. First we study the kink-profile type in (1.8)–(1.9) and also the local well-posedness problem associated to (2.1). Next, we apply the linear instability criterion (Theorem 2.4) to prove that the family of stationary solutions (1.8) are linearly (and nonlinearly) unstable (Theorem 1.1). Our second focus goes to the study of the anti-kink-profile type in (1.10) and similarly as in the former profile case we establish the necessary ingredients for obtaining Theorem 1.2.

3.1. Kink-profile's instability on a tricrystal junction

We start our stability study for the kink-profile type in (1.8)–(1.9) and so our first focus is dedicated to the Cauchy problem associated to the sine–Gordon model in (2.1). As this study is not completely standard in the case of metric graphs we provide the new ingredients that arise.

3.1.1. Cauchy Problem in $H^1(\mathcal{Y}) \times L^2(\mathcal{Y})$

In this subsection we establish the local well-posedness in $H^1(\mathcal{Y})\times L^2(\mathcal{Y})$ of the sine–Gordon equation on a tricrystal junction (section §2 in [10]). We start with the following result from the extension theory. The proof follows the same strategy as in Proposition A.6 and Theorem 3.1 in Angulo and Plaza [11] (see Proposition A.4 in the Appendix) and we omit it.

Proposition 3.1. *Consider the closed symmetric operator $(\mathcal{T}, D(\mathcal{T}))$ densely defined on $L^2(\mathcal{Y})$, with $\mathcal{Y}$ being a tricrystal junction, by*

$$\begin{aligned} \mathcal{T} &= \Big(\Big(-c_j^2\frac{d^2}{dx^2}\Big)\delta_{j,k}\Big), \quad 1 \leqq j,k \leqq 3, \\ D(\mathcal{T}) &= \Big\{ (v_j)_{j=1}^3 \in H^2(\mathcal{Y}) : c_1 v_1'(0+) = c_2 v_2'(0+) = c_3 v_3'(0+) = 0, \\ &\qquad \sum_{j=1}^3 c_j v_j(0+) = 0 \Big\}. \end{aligned} \tag{3.1}$$

Here $c_j \neq 0$, $1 \leqq j \leqq 3$, and $\delta_{j,k}$ is the Kronecker symbol. Then, the deficiency indices are $n_\pm(\mathcal{T}) = 1$. Therefore, we have that all the self-adjoint extensions of $(\mathcal{T}, D(\mathcal{T}))$ are given by the one-parameter family $(\mathcal{T}_\gamma, D(\mathcal{T}_\gamma))$, $\gamma \in \mathbb{R}$, with $\mathcal{T}_\gamma \equiv \mathcal{T}$ and $D(\mathcal{T}_\gamma)$ defined by

$$D(\mathcal{T}_\gamma) = \{(u_j)_{j=1}^3 \in H^2(\mathcal{Y}) : c_1 u_1'(0+) = c_2 u_2'(0+) = c_3 u_3'(0+),$$
$$\sum_{j=1}^3 c_j u_j(0+) = \gamma c_1 u_1'(0+)\}. \tag{3.2}$$

Moreover, the spectrum of the family of self-adjoint operators $(\mathcal{T}_\gamma, D(\mathcal{T}_\gamma))$ satisfies $\sigma_{\mathrm{ess}}(\mathcal{T}_\gamma) = [0, +\infty)$ for every $\gamma \neq 0$. For $\gamma < 0$, $\mathcal{T}_\gamma$ has precisely one negative simple eigenvalue. If $\gamma > 0$ then $\mathcal{T}_\gamma$ has no eigenvalues (see [8]).

Theorem 3.2. *Let $\mathcal{Y} = (0, +\infty) \cup (0, +\infty) \cup (0, +\infty)$. For any $\Psi \in H^1(\mathcal{Y}) \times L^2(\mathcal{Y})$ there exists $T > 0$ such that the sine–Gordon equation (2.1) has a unique solution $\mathbf{w} \in C([0,T]; H^1(\mathcal{Y}) \times L^2(\mathcal{Y}))$ satisfying $\mathbf{w}(0) = \Psi$. For each $T_0 \in (0,T)$ the mapping data-solution*

$$\Psi \in H^1(\mathcal{Y}) \times L^2(\mathcal{Y}) \to \mathbf{w} \in C([0,T_0]; H^1(\mathcal{Y}) \times L^2(\mathcal{Y})), \tag{3.3}$$

is at least of class C^2.

Proof. By applying the same strategy as in [10] (Theorems 2.2, 2.5 and 2.7) and [11] (Theorem 3.2), we have the following:

1. Consider the linear operators J and E defined in (2.2) with $(\mathcal{T}_\gamma, D(\mathcal{T}_\gamma))$ defined in Proposition 3.1. Then, $\mathcal{A} \equiv JE$ with $D(\mathcal{A}) = D(\mathcal{T}_\gamma) \times H^1(\mathcal{Y})$ is the infinitesimal generator of a C_0-semigroup on $X(\mathcal{Y}) \equiv H^1(\mathcal{Y}) \times L^2(\mathcal{Y})$.
2. By using the contraction mapping principle (Banach fixed point theorem), we obtain the local well-posedness result for the sine–Gordon equation (2.1) on $X(\mathcal{Y})$. We will give the sketch of the proof for convenience of the reader. Consider the mapping $J_\Psi : C([0,T] : X(\mathcal{Y})) \longrightarrow C([0,T]; X(\mathcal{Y}))$ given by
$$J_\Psi[\mathbf{w}](t) = e^{t\mathcal{A}}\Psi + \int_0^t e^{(t-s)\mathcal{A}} F(\mathbf{w}(s))ds,$$
where $e^{t\mathcal{A}}$ is the C_0-semigroup generated by $\mathcal{A}$. One needs to show that the mapping J_Ψ is well-defined. We note immediately that the nonlinearity satisfies for $\mathbf{w} = (\mathbf{u}, \mathbf{v}) \in X(\mathcal{Y})$ that $F(\mathbf{w}) \in X(\mathcal{Y})$ with $\|F(\mathbf{w})\|_{X(\mathcal{Y})} \leqq \|\mathbf{u}\|_{L^2(\mathcal{Y})} \leqq \|\mathbf{w}\|_{X(\mathcal{Y})}$. Thus we obtain for $t \in [0,T]$
$$\begin{aligned} &\|J_\Psi[\mathbf{w}](t)\|_{X(\mathcal{Y})} \\ &\quad \leq M e^{\gamma T}\|\Psi\|_{X(\mathcal{Y})} + \frac{M}{\gamma}\Big(e^{\gamma T} - 1\Big) \sup_{s\in[0,T]} \|\mathbf{w}(s)\|_{X(\mathcal{Y})}, \end{aligned}$$
where the positive constants M, γ do not depend on Ψ and are determined by the semigroup $e^{t\mathcal{A}}$. The continuity and contraction property of J_Ψ are proved in a standard way. Therefore, we obtain the existence of a unique solution to the Cauchy problem associated to (2.1) on $X(\mathcal{Y})$ and that the mapping data-solution in (3.3) is at least continuous.
Next, we recall that the argument based on the contraction mapping principle above has the advantage that if $F(\mathbf{w})$ has a specific regularity, then it is inherited by the mapping data-solution. In particular, following the ideas in [8], we consider for $(\Psi, \mathbf{z}) \in B(\Psi; \epsilon) \times C([0,T], X(\mathcal{Y}))$ the mapping
$$\Gamma(\Psi, \mathbf{z})(t) = \mathbf{z}(t) - J_\Psi[\mathbf{z}](t), \qquad t \in [0,T].$$
Then $\Gamma(\Psi, \mathbf{w})(t) = 0$ for all $t \in [0,T]$, and since $F(\mathbf{z})$ is smooth we obtain that Γ is smooth. Hence, using the arguments applied for obtaining the local well-posedness in $X(\mathcal{Y})$ above, we can show that the operator $\partial_{\mathbf{z}}\Gamma(\Psi, \mathbf{w})$ is one-to-one and onto. Thus, by the Implicit Function Theorem there exists a smooth mapping $\mathbf{\Lambda} : B(\Psi; \delta) \to C([0,T], X(\mathcal{Y}))$ such that $\Gamma(\mathbf{V}_0, \mathbf{\Lambda}(\mathbf{V}_0)) = 0$ for all $\mathbf{V}_0 \in B(\Psi; \delta)$. This argument establishes the smoothness property of the mapping data-solution associated to the sine–Gordon equation. □

We are ready to draw conclusions about the linearized operator $\mathcal{W}$ in (1.11) around the family of stationary solutions of the form (1.8) on a tricrystal junction required by the assumptions in Section 2. To denote the dependence of this operator on the parameter $\gamma \equiv \lambda$ in the case of the kink-type profile we write it as $(\mathcal{W}_\lambda, D(\mathcal{W}_\lambda))$. Moreover, by the results in Section 3.1.2, we shall consider $\lambda \in (-\infty, -\sum_{j=1}^3 c_j)$.

Proposition 3.3. *Consider the operator $(\mathcal{W}_\lambda, D(\mathcal{W}_\lambda))$ determined by $\mathcal{W}_\lambda \equiv \mathcal{W}$ defined in (1.11), on the domain $D(\mathcal{W}_\lambda) = D(\mathcal{T}_\lambda)$ defined in (3.2). Let $\mathcal{E}$ be the following diagonal-matrix*

$$\mathcal{E} = \begin{pmatrix} \mathcal{W}_\lambda & 0 \\ 0 & I_3 \end{pmatrix}.$$

Then $J\mathcal{E}$ is the generator of a C_0-semigroup on $H^1(\mathcal{Y}) \times L^2(\mathcal{Y})$ with $D(J\mathcal{E}) = D(\mathcal{W}_\lambda) \times H^1(\mathcal{Y})$. This implies, in turn, that assumption (S_1) (see Section 2) is satisfied.

Proof. From the relation $J\mathcal{E} = JE + \mathcal{Z}$ (see (2.9) for $\zeta_j = \varphi_j$), standard semigroup theory and item 1) in the proof of Theorem 3.2 imply the result. □

3.1.2. Kink-profile for the sine–Gordon equation on a tricrystal-junction

We will consider stationary solutions $(\varphi_j)_{j=1}^3$ for the sine–Gordon equation on a tricrystal-junction of the form (1.8) satisfying the δ'-interactions at the vertex given by (2.4), this means that $(\varphi_j)_{j=1}^3 \in D(\mathcal{T}_\lambda)$. Here we shall consider the *full continuity case* at the vertex, under which

$$\varphi_1(0+) = \varphi_2(0+) = \varphi_3(0+).$$

Hence $b_1/c_1 = b_2/c_2 = b_3/c_3$ and, moreover, the conditions $c_1\varphi_1'(0+) = c_2\varphi_2'(0+) = c_3\varphi_3'(0+)$ hold. The Kirchhoff type condition in (1.7) implies, for $y = e^{b_1/c_1}$, the relation

$$\frac{1+y^2}{y}\arctan(y)\sum_{j=1}^3 c_j = -\lambda. \tag{3.4}$$

Thus from the strictly-increasing property of the positive mapping $y \mapsto \frac{1+y^2}{y}\arctan(y)$, $y > 0$, we obtain from (3.4) that $\lambda \in (-\infty, -\sum_{j=1}^3 c_j)$ and the existence of a smooth mapping $\lambda \mapsto b_1(\lambda)$ satisfying (3.4). Moreover, $\lambda \in (-\infty, -\sum_{j=1}^3 c_j) \mapsto \Pi_{\lambda,\delta'} = (\varphi_{1,b_1(\lambda)}, \varphi_{2,b_2(\lambda)}, \varphi_{3,b_3(\lambda)}, 0, 0, 0)$ represents a real-analytic family of static profiles for the sine–Gordon equation on a tricrystal-junction. Thus, we have:

(1) for $\lambda \in (-\infty, -\frac{\pi}{2}\sum_{j=1}^3 c_j)$ we obtain that $b_i > 0$ and $\varphi_i''(b_i) = 0$, for every i. Moreover, $\varphi_i(0+) \in (\eta, 2\pi)$, $i = 1, 2, 3$, with $\eta = 4\arctan(e^{b_1/c_2}) > \pi$. Thus, the profile $(\varphi_1, \varphi_2, \varphi_3)$ looks like that presented in Fig. 2 (bump-type profile);
(2) for $\lambda \in (-\frac{\pi}{2}\sum_{j=1}^3 c_j, -\sum_{j=1}^3 c_j)$ we obtain $b_i < 0$, $\varphi_i'' > 0$, $\varphi_i \in (0, \pi)$ for every i. Thus, the profile $(\varphi_1, \varphi_2, \varphi_3)$ is of tail-type as that of Fig. 2(b);
(3) for $\lambda = -\frac{\pi}{2}\sum_{j=1}^3 c_j$ we obtain $b_i = 0$, $\varphi_i(0) = \pi$ and $\varphi_i''(0) = 0$, for every i. Moreover, $\varphi_i''(x) > 0$ for $x > 0$. Thus, the profile $(\varphi_1, \varphi_2, \varphi_3)$ is similar to that of Fig. 2(c).

The stability result for the stationary profiles, $\Pi_{\lambda,\delta'} = (\varphi_1, \varphi_2, \varphi_3, 0, 0, 0)$, with $\varphi_j = \varphi_{j,b_j(\lambda)}$ defined in (1.8) and (3.4) in the continuous case is that established in Theorem 1.1. We leave for a possible future study the stability analysis of other kink-type profiles, such as those non-continuous at the vertex.

The proof of Theorem 1.1 is a consequence of Theorem 2.4. Thus we only need to verify assumption (S_3) associated to the family of self-adjoint operators $\mathcal{W}_\lambda$ in (1.11) (see Proposition 3.1), with the domain $D(\mathcal{W}_\lambda) = D(\mathcal{T}_\lambda)$ in (3.2) and the kink-profiles φ_j defined in (1.8).

3.1.3. Spectral study for $(\mathcal{W}_\lambda, D(\mathcal{W}_\lambda))$ on a tricrystal-junction

In this subsection, the spectral behavior for $\mathcal{W}_\lambda$ on $D(\mathcal{W}_\lambda)$ will be studied, with the focus on verifying assumption (S_3) in Section 2.

Proposition 3.4. *Let $\lambda \in (-\infty, -\sum_{j=1}^3 c_j)$, $c_j > 0$. Then for $\lambda \neq -\frac{\pi}{2}\sum_{j=1}^3 c_j$ we have $\ker(\mathcal{W}_\lambda) = \{\mathbf{0}\}$. For $\lambda_0 = -\frac{\pi}{2}\sum_{j=1}^3 c_j$, $\dim(\ker(\mathcal{W}_{\lambda_0})) = 2$. Moreover, $\sigma_{\mathrm{ess}}(\mathcal{W}_\lambda) = [1, +\infty)$.*

Proof. We consider $\mathbf{u} = (u_1, u_2, u_3) \in D(\mathcal{W}_\lambda)$ and $\mathcal{W}_\lambda\mathbf{u} = \mathbf{0}$. Then, from Sturm–Liouville theory on half-lines (see [46], Chapter 2, Theorem 3.3), $u_j(x) = \alpha_j\varphi_j'(x)$, $x > 0$, $j = 1, 2, 3$. Thus, for $\lambda \neq -\frac{\pi}{2}\sum_{j=1}^3 c_j$ we obtain $\alpha_1/c_1 = \alpha_2/c_2 = \alpha_3/c_3$. Next, from the jump conditions for $\mathbf{u}$ and $\Psi_{\lambda,\delta'} = (\varphi_j)$, we obtain

$$\alpha_1\varphi_1'(0)\sum_{j=1}^3 c_j = \alpha_1\lambda c_1\varphi_1''(0). \tag{3.5}$$

Next, suppose $\alpha_1 \neq 0$. Since $\varphi_1'(0) < 0$ and for $\lambda \in (-\infty, -\frac{\pi}{2}\sum_{j=1}^3 c_j)$ we have $\varphi_1''(0) < 0$, relation in (3.5) implies a contradiction because of $c_j > 0$. Now, considering $\lambda \in (-\frac{\pi}{2}\sum_{j=1}^3 c_j, -\sum_{j=1}^3 c_j)$ and from the specific values of $\varphi_1'(0)$, $\varphi_1''(0)$ we obtain from (3.5) again a contradiction. Thus, from the two cases above we need to have $\alpha_1 = \alpha_2 = \alpha_3 = 0$. For $\lambda_0 = -\frac{\pi}{2}\sum_{j=1}^3 c_j$ we recall that $\varphi_j''(0) = 0$ for every j. Hence, from the jump-condition for $\mathbf{u}$ follows $\sum_{j=1}^3 \alpha_j = 0$. Then $\Psi_1 = (\varphi_1', -\varphi_2', 0)$ and $\Psi_2 = (0, \varphi_2', -\varphi_3')$ belong to $D(\mathcal{W}_{\lambda_0})$ and $\mathrm{span}\{\Psi_1, \Psi_2\} = \ker(\mathcal{W}_{\lambda_0})$.

The statement $\sigma_{\mathrm{ess}}(\mathcal{W}_\lambda) = [1, +\infty)$ is an immediate consequence of Weyl's Theorem because of $\lim_{x\to+\infty}\cos(\varphi_j(x)) = 1$ (see [47]). This finishes the proof. □

Proposition 3.5. *Let $\lambda \in [-\frac{\pi}{2}\sum_{j=1}^3 c_j, -\sum_{j=1}^3 c_j)$. Then $n(\mathcal{W}_\lambda) = 1$.*

Proof. We will use the extension theory approach, which is based on the fact that the family $(\mathcal{W}_\lambda, D(\mathcal{W}_\lambda))$ represents all the self-adjoint extensions of the closed symmetric operator $(\widetilde{T}, D(\widetilde{T}))$ with $D(\widetilde{T}) \equiv D(\mathcal{T})$ defined in (3.1), and

$$\widetilde{T} = \left(\left(-c_j^2\frac{d^2}{dx^2} + \cos(\varphi_j)\right)\delta_{j,k}\right), \ \ 1 \leqq j, k \leqq 3, \tag{3.6}$$

with $n_\pm(\widetilde{T}) = 1$. Next, we show that $\widetilde{T} \geqq 0$. If we denote $L_j = -c_j^2\frac{d^2}{dx^2} + \cos(\varphi_j)$ then we obtain

$$L_j\psi = -\frac{1}{\varphi_j'}\frac{d}{dx}\left[c_j^2(\varphi_j')^2\frac{d}{dx}\left(\frac{\psi}{\varphi_j'}\right)\right], \tag{3.7}$$

for any ψ. It is to be observed that $\varphi_j' \neq 0$. Then we have for any $\Lambda = (\psi_j) \in D(\widetilde{T})$ and integration by parts the relation

$$\begin{aligned}\langle \widetilde{T}\Lambda, \Lambda\rangle &= \sum_{j=1}^3 c_j^2\int_0^{+\infty}(\varphi_j')^2\left(\frac{d}{dx}\left(\frac{\psi}{\varphi_j'}\right)\right)^2 dx \\ &\quad - \sum_{j=1}^3 c_j^2\psi_j^2(0)\frac{\varphi_j''(0)}{\varphi_j'(0)} \equiv A + P,\end{aligned} \tag{3.8}$$

where $A \geqq 0$ represents the integral terms. Next we show that $P \geqq 0$. Indeed, since $\varphi_j''(0) \geqq 0$ and $\varphi_j'(0) < 0$, for $j = 1, 2, 3$, we obtain immediately $P \geqq 0$. Then, $\widetilde{T} \geqq 0$.

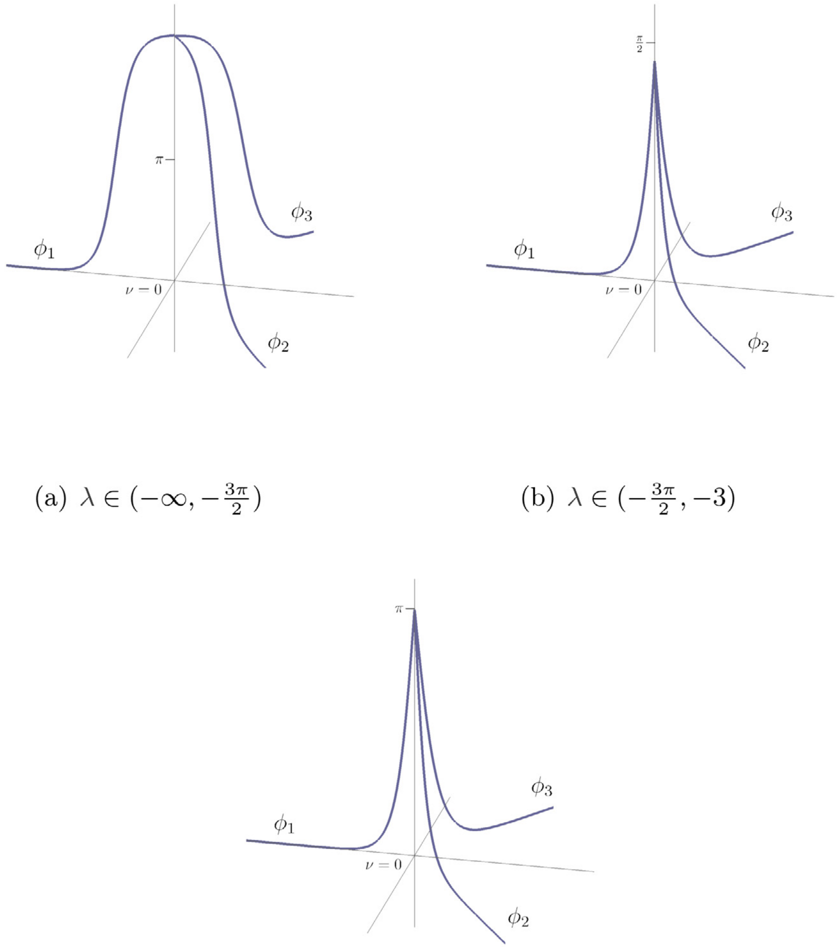

(a) $\lambda \in (-\infty, -\frac{3\pi}{2})$

(b) $\lambda \in (-\frac{3\pi}{2}, -3)$

(c) $\lambda = -\frac{3\pi}{2}$

Fig. 2. Plots of stationary solutions (1.8) in the case where $c_j = 1$ for all $j = 1, 2, 3$, for different values of $\lambda \in (\infty, -\sum_j c_j) = (-\infty, -3)$. Panel (a) shows the stationary profile solutions ("bump" configuration) for the case $\lambda \in (-\infty, -\frac{3\pi}{2})$. Panel (b) shows the profiles of "tail" type for the case $\lambda \in (-\frac{3\pi}{2}, -3)$. Panel (c) shows the "smooth" profile solutions when $\lambda = -\frac{3\pi}{2}$ (color online).

Due to Proposition A.3 (see Appendix), $n(\mathcal{W}_\lambda) \leqq 1$. Next, for $\Psi_{\lambda,\delta'} = (\varphi_1, \varphi_2, \varphi_3) \in D(\mathcal{W}_\lambda)$ we obtain

$$\langle \mathcal{W}_\lambda \Psi_{\lambda,\delta'}, \Psi_{\lambda,\delta'} \rangle = \sum_{j=1}^{3} \int_0^{+\infty} [-\sin(\varphi_j) + \cos(\varphi_j)\varphi_j]\varphi_j dx < 0, \quad (3.9)$$

because of $0 < \varphi_j(x) \leqq \pi$ and $x \cos x \leqq \sin x$ for all $x \in [0, \pi]$. Then from the minimax principle (see, e.g., [47], p. 76) we arrive at $n(\mathcal{W}_\lambda) \geqq 1$. This finishes the proof. □

Proof of Theorem 1.1. Let $\lambda \in (-\frac{\pi}{2} \sum_{j=1}^3 c_j, -\sum_{j=1}^3 c_j)$. Then, from Propositions 3.4 and 3.5 we have $\ker(\mathcal{W}_\lambda) = \{0\}$ and $n(\mathcal{W}_\lambda) = 1$. Thus, from Theorem 3.2, Proposition 3.3 and Theorem 2.4 follow the linear instability property of the stationary profile $\Pi_{\lambda,\delta'} = (\varphi_1, \varphi_2, \varphi_3, 0, 0, 0)$.

Next, we consider the closed subspace in $L^2(\mathcal{Y})$, $\mathcal{C}_1 = \{(u_j)_{j=1}^3 \in L^2(\mathcal{Y}) : u_1 = u_2 = u_3\}$, and the case $c_1 = c_2 = c_3$ (hence $b_1 = b_2 = b_3$). Then, we can show that on $\mathcal{B}_1 = \mathcal{C}_1 \cap D(\mathcal{W}_\lambda)$ we obtain $\mathcal{W}_\lambda : \mathcal{B}_1 \to \mathcal{C}_1$ is well-defined. Moreover, we note that for $\lambda_0 = -\frac{\pi}{2} \sum_{j=1}^3 c_j$ follows $\ker(\mathcal{W}_{\lambda_0}|_{\mathcal{B}_1}) = \{\mathbf{0}\}$ and $n(\mathcal{W}_{\lambda_0}|_{\mathcal{B}_1}) = 1$ (because $\Psi_{\lambda_0,\delta'} = (\varphi_1, \varphi_1, \varphi_1) \in \mathcal{B}_1$ and $\langle \mathcal{W}_{\lambda_0} \Psi_{\lambda_0,\delta'}, \Psi_{\lambda_0,\delta'} \rangle < 0$). Therefore, from Kato–Rellich Theorem, analytic perturbation and a continuation argument (see [8–10,48,49] and/or Propositions 3.10 and 3.11), we can see that for all $\lambda \in (-\infty, -\frac{\pi}{2} \sum_{j=1}^3 c_j]$ the following relations hold: $\ker(\mathcal{W}_\lambda|_{\mathcal{B}_1}) = \{\mathbf{0}\}$ and $n(\mathcal{W}_\lambda|_{\mathcal{B}_1}) = 1$. Thus, the static profiles $\Pi_{\lambda,\delta'}$ are also linearly unstable in this case.

Now, since the mapping data-solution for the sine–Gordon model on $H^1(\mathcal{Y}) \times L^2(\mathcal{Y})$ is at least of class C^2 (indeed, it is smooth) by Theorem 3.2, it follows that the linear instability property of $\Psi_{\lambda,\delta'}$ is in fact of nonlinear type in the $H^1(\mathcal{Y}) \times L^2(\mathcal{Y})$-norm (see Henry et al. [50], Angulo and Natali [49], and Angulo et al. [48]). This finishes the proof. □

Remark 3.6. For the case $\lambda \in (-\infty, -\frac{\pi}{2} \sum_{j=1}^3 c_j)$ in Proposition 3.5, the formula for P in (3.8) satisfies $P < 0$. Therefore, it is not clear whether the extension theory approach provides an estimate of the Morse-index of $\mathcal{W}_\lambda$; see also the related Remark 4.5 in [10]. Likewise, in the case $\lambda \in (-\infty, -\frac{\pi}{2} \sum_{j=1}^3 c_j)$ with all c_j's not equal, the Morse index may change and to be bigger than or equal to 2, consequently, the stability properties may change as well; see the related Remark 3.15 in [11].

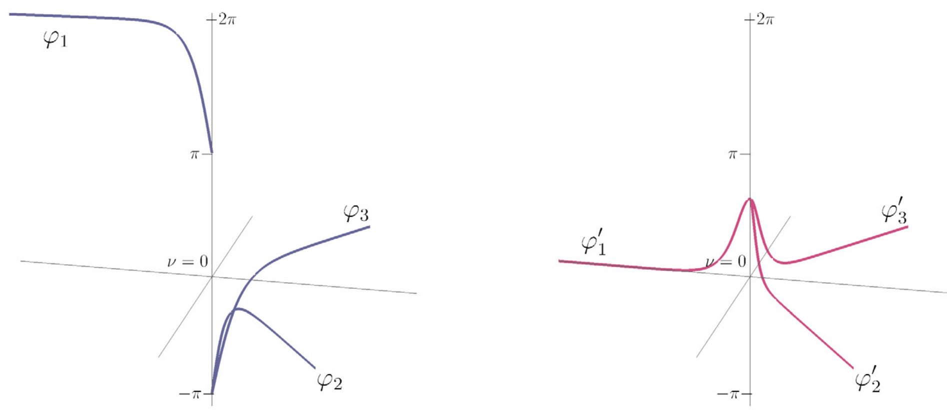

(a) Kink/anti-kink profiles, φ_j. (b) "Fluxons", φ_j'.

Fig. 3. Plots of the kink/anti-kink profiles (1.10) (panel (a), in blue) and their corresponding derivatives or "fluxons" (panel (b), in red) in the case where $c_j = 1$, $a_j = 0$, $j = 1, 2, 3$, and $Z = -\frac{\pi}{2}(c_2 + c_3 - c_1) = -\frac{\pi}{2}$. Both plots are depicted in the same scale for comparison purposes. (For interpretation of the references to color in this figure legend, the reader is referred to the web version of this article.)

3.2. Kink/anti-kink instability theory on a tricrystal junction

In this subsection we study the existence and stability of kink/anti-kink profile in (1.10). Since these stationary profiles do not belong to the classical $H^2(\mathcal{Y})$- space, we need to work with specific functional spaces suitable for our needs.

3.2.1. The anti-kink/kink solutions on a tricrystal junction

In the sequel, we describe the profiles $(\varphi_j)_{j=1}^3$ in (1.10) satisfying the δ'-condition in (1.7) with $\gamma = Z$. Thus, we obtain the following relations:

$$\operatorname{sech}\Big(\frac{a_1}{c_1}\Big) = \operatorname{sech}\Big(\frac{a_2}{c_2}\Big) = \operatorname{sech}\Big(\frac{a_3}{c_3}\Big), \tag{3.10}$$

and

$$\begin{aligned} &c_1 \arctan(e^{-a_1/c_1}) + c_2 \arctan(e^{-a_2/c_2}) + c_3 \arctan(e^{-a_3/c_3}) \\ &\quad - \frac{(c_2 + c_3)\pi}{2} = \frac{Z}{2} \operatorname{sech}\Big(\frac{a_1}{c_1}\Big). \end{aligned} \tag{3.11}$$

Here, we consider the specific class of anti-kink/kink profiles with the condition $\frac{a_1}{c_1} = \frac{a_2}{c_2} = \frac{a_3}{c_3}$. Thus, from (3.11) and $y = e^{-a_1/c_1}$ we get the following equality

$$F(y) \equiv \frac{1 + y^2}{y}\Big[\Big(\sum_{i=1}^{3} c_i\Big) \arctan(y) - \frac{(c_2 + c_3)\pi}{2}\Big] = Z. \tag{3.12}$$

Next, we show that the mapping F is strictly increasing for $y > 0$. Indeed, since for $y \in (0, 1)$ we have that $\frac{1}{y} + \frac{y^2-1}{y^2} \arctan(y) > 0$, then $F'(y) > 0$. Now, for $\theta = \sum_{i=1}^{3} c_i$, the relation

$$\begin{aligned} F'(y) &= \theta\Big[\frac{1}{y} + \frac{y^2 - 1}{y^2}\Big(\arctan(y) - \frac{\pi}{2}\Big)\Big] \\ &\quad + \theta\Big[\frac{\pi}{2} - \frac{(c_2 + c_3)\pi}{2\sum_{i=1}^{3} c_i}\Big]\frac{y^2 - 1}{y^2} \end{aligned} \tag{3.13}$$

shows that $F'(y) > 0$ for $y \in [1, +\infty)$. Moreover, it is no difficult to see that $\lim_{y\to 0^+} F(y) = -\infty$, and $\lim_{y\to +\infty} F(y) = +\infty$.

Then, from (3.12) we have the following specific behavior of the Z-parameter:

(a) for $a_1 = 0$, $Z = -\frac{\pi}{2}(c_2 + c_3 - c_1)$,
(b) for $a_1 > 0$, $Z \in (-\infty, -\frac{\pi}{2}(c_2 + c_3 - c_1))$,
(c) for $a_1 < 0$, $Z \in (-\frac{\pi}{2}(c_2 + c_3 - c_1), +\infty)$.

Moreover, from (3.12) and the properties for F we obtain the existence of a smooth shift-map (also real analytic) $Z \in (-\infty, +\infty) \mapsto a_1(Z)$ satisfying $F(e^{-a_1(Z)/c_1}) = Z$. Thus, the mapping

$$Z \in (-\infty, +\infty) \mapsto \Phi_{Z,\delta'} = (\varphi_{1,a_1(Z)}, \varphi_{2,a_2(Z)}, \varphi_{3,a_3(Z)}, 0, 0, 0),$$

represents a real-analytic family of static profiles for the sine–Gordon equation (1.5) on a tricrystal junction, with the profiles $\varphi_{j,a_j(Z)}$ satisfying the boundary condition in (1.10). Hence we obtain, for $a_i = a_i(Z)$ and $\varphi_i = \varphi_{i,a_i(Z)}$, the following behavior:

(1) for $Z = -\frac{\pi}{2}(c_2 + c_3 - c_1)$ we obtain $a_1 = a_2 = a_3 = 0$, $\varphi_2(0) = \varphi_3(0) = -\pi$, $\varphi_1(0) = \pi$, $\varphi_i''(0) = 0$, $i = 1, 2, 3$. Thus, the profile of $(\varphi_1, \varphi_2, \varphi_3)$ represents one-half positive anti-kink φ_1 and two-half negative kink solitons profiles φ_2, φ_3 (connected in the vertex of the graph) such as Fig. 3 shows below;
(2) for $Z \in (-\infty, -\frac{\pi}{2}(c_2 + c_3 - c_1))$ we obtain $a_1 > 0$, $\varphi_i''(a_1) = 0$, $i = 1, 2, 3$. Therefore, $\varphi_1(0) \in (0, \pi)$ and $\varphi_2(0) = \varphi_3(0) \in (-\pi, -2\pi)$. Thus, the profile of $(\varphi_1, \varphi_2, \varphi_2)$, looks similar to the one shown in Fig. 4 (bump-profile type);
(3) for $Z \in (-\frac{\pi}{2}(c_2 + c_3 - c_1), +\infty)$ we obtain $a_1 < 0$ and therefore $\varphi_i'' < 0$ for $i = 1, 2, 3$, Thus, the profile of $(\varphi_1, \varphi_2, \varphi_3)$ looks similar to that in Fig. 5 (typical tail-profile).

Here, our instability study of anti-kink/kink profiles will be in the case where the "magnetic field" or "fluxon" is continuous at the vertex of the tricrystal, namely, whenever $\varphi_1'(0) = \varphi_2'(0) = \varphi_3'(0)$ ($c_1 = c_2 = c_3$). It is to be observed that we have left open a possible instability study of other anti-kink/kink soliton configurations, for instance, profiles not satisfying the continuity property at zero for the components φ_2, φ_3 ($\frac{a_2}{c_2} \neq \frac{a_3}{c_3}$) and/or the non-continuity of the magnetic field.

The stability result for the stationary profiles, $\Phi_{Z,\delta'} = (\varphi_1, \varphi_2, \varphi_3, 0, 0, 0)$, with $\varphi_j = \varphi_{j,a_j(Z)}$ defined in (1.10) is that established in Theorem 1.2.

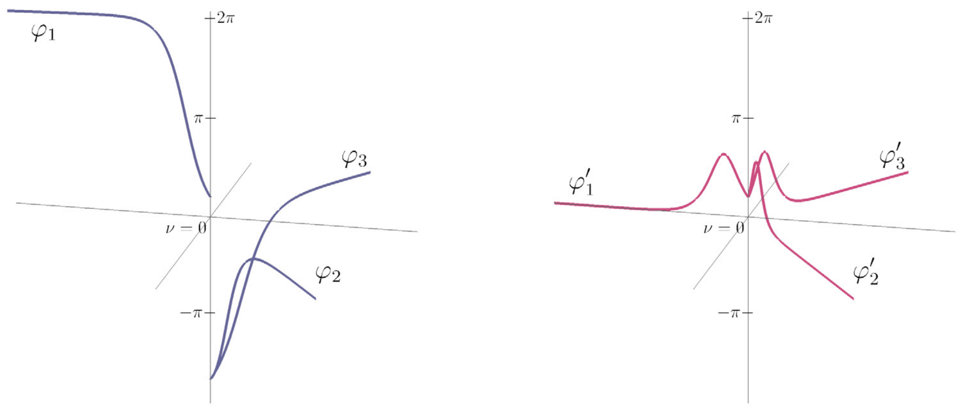

(a) Kink/anti-kink profiles, φ_j. (b) "Fluxons", φ_j'.

Fig. 4. Plots of the kink/anti-kink profiles (1.10) (panel (a), in blue) and their corresponding derivatives or "fluxons" (panel (b), in red) in the case where $c_j = 1$, $a_j = 1.8 > 0$, $j = 1, 2, 3$, and $Z \in (-\infty, -\frac{\pi}{2})$. Both plots are depicted in the same scale for comparison purposes. (For interpretation of the references to color in this figure legend, the reader is referred to the web version of this article.)

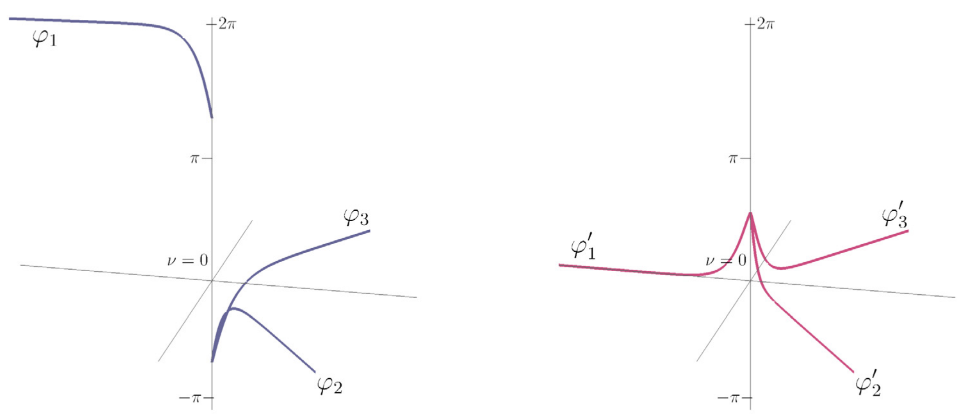

(a) Kink/anti-kink profiles, φ_j. (b) "Fluxons", φ_j'.

Fig. 5. Plots of the kink/anti-kink profiles (1.10) (panel (a), in blue) and their corresponding derivatives or "fluxons" (panel (b), in red) in the case where $c_j = 1$, $a_j = -0.5 < 0$, $j = 1, 2, 3$, and $Z \in (-\frac{\pi}{2}, \infty)$. Both plots are depicted in the same scale for comparison purposes. (For interpretation of the references to color in this figure legend, the reader is referred to the web version of this article.)

3.2.2. Functional space for stability properties of the anti-kink/kink profile

The natural framework space for studying stability properties associated to the anti-kink/kink soliton profile $\Phi = (\varphi_j)_{j=1}^3$ described in the former subsection for the sine–Gordon model is $\mathcal{X}(\mathcal{Y}) = H^1_{\text{loc}}(0,\infty) \bigoplus H^1(0,\infty) \bigoplus H^1(0,\infty)$. Thus we say that a flow $t \to (u(t), v(t)) \in \mathcal{X}(\mathcal{Y}) \times L^2(\mathcal{Y})$ is called a *perturbed solution* for the anti-kink/kink profile $\Phi \in \mathcal{X}(\mathcal{Y})$ if for $(P(t), Q(t)) \equiv (u(t) - \Phi, v(t))$ we have that $(P(t), Q(t)) \in H^1(\mathcal{Y}) \times L^2(\mathcal{Y})$ and $\mathbf{z} = (P, Q)^\top$ satisfies the following vectorial perturbed sine–Gordon model

$$\begin{cases} \mathbf{z}_t = JE\mathbf{z} + F_1(\mathbf{z}) \\ P(0) = u(0) - \Phi \in H^1(\mathcal{Y}), \\ Q(0) = v(0) \in L^2(\mathcal{Y}), \end{cases} \tag{3.14}$$

where for $P = (p_1, p_2, p_3)$ we have

$$F_1(\mathbf{z}) = \begin{pmatrix} 0 \\ 0 \\ 0 \\ \sin(\varphi_1) - \sin(p_1 + \varphi_1) \\ \sin(\varphi_2) - \sin(p_2 + \varphi_2) \\ \sin(\varphi_3) - \sin(p_3 + \varphi_3) \end{pmatrix}. \tag{3.15}$$

Then, the stability analysis of the stationary anti-kink/kink $\Phi_{Z,\delta'} = (\varphi_1, \varphi_2, \varphi_3, 0, 0, 0)$ by the sine–Gordon model on $\mathcal{X}(\mathcal{Y}) \times L^2(\mathcal{Y})$ reduces to studying the stability properties of the trivial solution $(P, Q) = (0, 0)$ for the linearized model associated to (3.14) around $(P, Q) = (0, 0)$. Thus, via Taylor's Theorem we obtain the linearized system in (2.7) but with the Schrödinger diagonal operator $\mathcal{L}$ in (2.8) now determined by the anti-kink/kink profile $\Phi = (\varphi_j)$. We denote this operator by $\mathcal{L}_Z$ in (3.16), with the δ'-interaction domain $D(\mathcal{L}_Z)$ in (2.4). In this form, we can apply *ipsis litteris* the semi-group theory results in Section 3.1.1 to the operator JE and to the local well-posedness problem in $H^1(\mathcal{Y}) \times L^2(\mathcal{Y})$ for the vectorial perturbed sine–Gordon model (3.14). Lastly, we note that the anti-kink/kink profile $\Phi \in \mathcal{X}(\mathcal{Y})$, but $\Phi' \in H^2(\mathcal{Y})$.

3.2.3. The spectral study in the anti-kink/kink case

In this subsection we provide the necessary spectral information for the family of self-adjoint operators $(\mathcal{L}_Z, D(\mathcal{L}_Z))$, where

$$\mathcal{L}_Z = \left(\left(-c_j^2 \frac{d^2}{dx^2} + \cos(\varphi_j)\right)\delta_{j,k}\right), \quad 1 \leqq j, k \leqq 3, \tag{3.16}$$

associated to the anti-kink/kink solutions $(\varphi_1, \varphi_2, \varphi_3)$ determined in the previous Section 3.2.1 and depending of the parameter Z. Here, by convenience of the reader, we are using the notation $\mathcal{L}_Z \equiv \mathcal{W}$ in (1.11) in order not to cause any confusion with the notation $\mathcal{W}_\lambda$ in the previous subsection associated to the kink-profile (1.8), and $D(\mathcal{L}_Z)$ is now the δ'-interaction domain defined in (1.12) for $\gamma = Z \in (-\infty, \infty)$.

By completeness and convenience of the reader, we prove the following result associated to the kernel of the operators $\mathcal{L}_Z$ for all values of c_1, c_2, c_3 and the admissible Z-values. We note that this result is expected, due to the break in the translation symmetry of solutions for the sine–Gordon model on tricrystal configurations. When one computes the Morse index of $\mathcal{L}_Z$, however, the study is more delicate and we restrict the analysis to the case $c_1 = c_2 = c_3$. This restriction is due to the possibility of obtaining a Morse index bigger than or equal to two (we call the attention to Proposition 3.11 and Remark 3.12).

Proposition 3.7. *Let $c_1, c_2, c_3 > 0$ and $Z \in (-\infty, \infty)$. Then, $\ker(\mathcal{L}_Z) = \{\mathbf{0}\}$ for all $Z \neq -\frac{\pi}{2}(c_2+c_3-c_1)$. For $Z = -\frac{\pi}{2}(c_2+c_3-c_1)$ we have $\dim(\ker(\mathcal{L}_Z)) = 2$. Moreover, for all Z we obtain $\sigma_{\text{ess}}(\mathcal{L}_Z) = [1, \infty)$.*

Proof. Let $\mathbf{u} = (u_1, u_2, u_3) \in D(\mathcal{L}_Z)$ and $\mathcal{L}_Z\mathbf{u} = \mathbf{0}$. Then, since $(\varphi_1', \varphi_3', \varphi_2') \in H^2(\mathcal{Y})$, it follows from Sturm–Liouville theory on half-lines that

$$u_j(x) = \alpha_j \phi_j'(x), \quad x > 0, \quad j = 1, 2, 3, \tag{3.17}$$

for some α_j, $j = 1, 2, 3$, real constant. In what follows, we assume $Z \neq -\frac{\pi}{2}(c_2 + c_3 - c_1)$. Thus, from (2.4) and by supposing $\alpha_1 \neq 0$ we have

$$\frac{\alpha_2}{\alpha_1} = \frac{c_1}{c_2}\frac{\varphi_1''(0)}{\varphi_2''(0)} = \frac{c_2}{c_1}, \qquad \frac{\alpha_3}{\alpha_1} = \frac{c_1}{c_3}\frac{\varphi_1''(0)}{\varphi_3''(0)} = \frac{c_3}{c_1} \tag{3.18}$$

and

$$Z = \frac{1}{\alpha_1}\left(\sum_{j=1}^{3} \alpha_j\right)\frac{\varphi_1'(0)}{\varphi_1''(0)} = (c_1 + c_2 + c_3)\frac{\cosh^2(a_1/c_1)}{\sinh(a_1/c_1)}. \tag{3.19}$$

Now, we consider the following cases:

(a) Suppose $a_1 < 0$ ($Z \in (-\frac{\pi}{2}(c_2 + c_3 - c_1), +\infty)$): then, since

$$\frac{\cosh^2(a_1/c_1)}{\sinh(a_1/c_1)} \leqq -2, \quad \text{for all} \quad a_1 < 0, \tag{3.20}$$

we have, from (3.19), $-\frac{\pi}{2}(c_2 + c_3 - c_1) < -2(c_1 + c_2 + c_3)$, which is a contradiction. So, we need to have $0 = \alpha_1 = \alpha_2 = \alpha_3$ and therefore $\mathbf{u} = \mathbf{0}$.

(b) Suppose $a_1 > 0$ ($Z \in (-\infty, -\frac{\pi}{2}(c_2 + c_3 - c_1))$: then, from (3.19) we have $Z > 2(c_1 + c_2 + c_3)$. Thus for the case $c_2 + c_3 - c_1 \geqq 0$ we obtain immediately a contradiction. Now, for $c_2 + c_3 - c_1 < 0$ is sufficient to study the case $0 < Z < -\frac{\pi}{2}(c_2 + c_3 - c_1)$. Indeed, since $2(c_1 + c_2 + c_3) > -\frac{\pi}{2}(c_2+c_3-c_1)$ we have again a contradiction. So, we need to have $0 = \alpha_1 = \alpha_2 = \alpha_3$ and therefore $\mathbf{u} = \mathbf{0}$.

Now, suppose that $Z = -\frac{\pi}{2}(c_2 + c_3 - c_1)$. In this case the Kirchhoff's condition for $\mathbf{u}$, $\varphi_1'(0) \neq 0$ and $\varphi_1''(0) = 0$ we get the relation $\alpha_1 + \alpha_2 + \alpha_3 = 0$. Therefore

$$(u_1, u_2, u_3) = \alpha_2(-\varphi_1', \varphi_2', 0) + \alpha_3(-\varphi_1', 0, \varphi_3').$$

Since $(-\varphi_1', \varphi_2', 0), (-\varphi_1', 0, \varphi_3') \in D(\mathcal{L}_Z)$ we obtain that $\dim(\ker(\mathcal{L}_Z)) = 2$.

The statement $\sigma_{\text{ess}}(\mathcal{L}_Z) = [1, +\infty)$ is an immediate consequence of Weyl's Theorem because of $\lim_{x\to+\infty} \cos(\varphi_1(x)) = 1 = \lim_{x\to+\infty} \cos(\varphi_j(x))$. This finishes the proof. $\square$

Proposition 3.8. *Let $c_1 = c_2 = c_3$ and $Z \in [-\frac{\pi}{2}c_1, 0)$. Then $n(\mathcal{L}_Z) = 1$.*

Proof. Similarly as in the proof of Proposition 3.5 (see formula (3.8)), we obtain via the extension theory that $n(\mathcal{L}_Z) \leqq 1$ for all $Z \in [-\frac{\pi}{2}c_1, +\infty)$ because of $\varphi_j''(0) \leqq 0$ for $j = 1, 2, 3$.

Now we show that $n(\mathcal{L}_Z) \geqq 1$ for $Z \in [-\frac{\pi}{2}c_1, 0)$. Indeed, we consider the following quadratic form $\mathcal{Q}_Z$ associated to $(\mathcal{L}_Z, D(\mathcal{L}_Z))$ for $\Lambda = (\psi_i) \in H^1(\mathcal{Y})$,

$$\mathcal{Q}(\Lambda) = \frac{1}{Z}\left(\sum_{j=1}^{3} c_j\psi_j(0)\right)^2 + \sum_{j=1}^{3}\int_0^\infty c_j^2(\psi_j')^2 + \cos(\varphi_j)\psi_j^2 dx. \tag{3.21}$$

Next, for $\Lambda_1 = (\varphi_1', \varphi_2', \varphi_3') \in H^1(\mathcal{Y})$ we obtain from the equalities $-\varphi_j''' + \cos(\varphi_j)\varphi_j' = 0$, $c_1\varphi_1'(0) = c_2\varphi_2'(0) = c_3\varphi_3'(0)$, and from integration by parts, the relation

$$\mathcal{Q}_Z(\Lambda_1) = \frac{9c_1^2}{Z}[\varphi_1'(0)]^2 - c_1\varphi_1'(0)\sum_{j=1}^{3} c_j\varphi_j''(0). \tag{3.22}$$

Thus, for $Z = -\frac{\pi}{2}c_1$ we have $\varphi_j''(0) = 0$ and therefore $\mathcal{Q}_Z(\Lambda_1) < 0$. Thus $n(\mathcal{L}_{-\frac{\pi}{2}c_1}) = 1$. Now, for $Z \in (-\frac{\pi}{2}c_1, 0)$ we have $\varphi_1''(0) < 0$ ($a_1 < 0$) and so since $\varphi_1''(0) = \varphi_2''(0) = \varphi_3''(0)$ we get $\mathcal{Q}_Z(\Lambda_1) < 0$ if and only if

$$3\frac{\varphi_1'(0)}{\varphi_1''(0)} = 3c_1\frac{\cosh^2(a_1)}{\sinh(a_1)} < Z, \quad \text{for} \quad a_1 < 0, \tag{3.23}$$

which is true by (3.20). Therefore, $n(\mathcal{L}_Z) = 1$ for $Z \in (-\frac{\pi}{2}c_1, 0)$. $\square$

Remark 3.9. For the case $Z \in [0, +\infty)$ in Proposition 3.8, it was not possible to show (in an easy way) that the quadratic form $\mathcal{Q}_Z$ in (3.21) has a negative direction. But we will see in the following, via analytic perturbation approach, that we still have $n(\mathcal{L}_Z) = 1$.

Proposition 3.10. *Let $c_1 = c_2 = c_3$ and $Z \in [0, +\infty)$. Then $n(\mathcal{L}_Z) = 1$.*

Proof. We will use analytic perturbation theory. Initially, from Section 3.2.1 we have that $Z \in (-\infty, +\infty) \to a_1(Z)$ represents a real-analytic mapping function and so from the relations $\varphi_{1,a_1(Z)} - \varphi_{1,a_1(0)} \in L^2(0, +\infty)$ for every Z and $\|\varphi_{1,a_1(Z)} - \varphi_{1,a_1(0)}\|_{H^1(0,+\infty)} \to 0$ as $Z \to 0$, we obtain for $\Phi_{a_1(Z)} = (\varphi_{1,a_1(Z)}, \varphi_{3,a_1(Z)}, \varphi_{2,a_1(Z)})$ (where we have used that $a_1(Z) = a_2(Z) = a_3(Z)$) the convergence

$$\|\Phi_{a_1(Z)} - \Phi_{a_1(0)}\|_{H^1(\mathcal{Y})} \to 0 \quad \text{as} \quad Z \to 0.$$

Thus, we obtain that $\mathcal{L}_Z$ converges to $\mathcal{L}_0$ as $Z \to 0$ in the generalized sense. Indeed, denoting $W_Z = \left(\cos(\varphi_{j,a_1(Z)})\delta_{j,k}\right)$ we obtain

$$\widehat{\delta}(\mathcal{L}_Z, \mathcal{L}_0) = \widehat{\delta}(\mathcal{L}_0 + (W_Z - W_0), \mathcal{L}_0) \leqq \|W_Z - W_0\|_{L^2(\mathcal{Y})} \to 0, \quad \text{as } Z \to 0,$$

where $\widehat{\delta}$ is the gap metric (see [51, Chapter IV]).

Now, we denote by $N = n(\mathcal{L}_0)$ the Morse-index for $\mathcal{L}_0$ (from the proof of Proposition 3.8, $N \leqq 1$). Thus, from Proposition 3.7 we can separate the spectrum $\sigma(\mathcal{L}_0)$ of $\mathcal{L}_0$ into two parts, $\sigma_0 = \{\gamma : \gamma < 0\} \cap \sigma(\mathcal{L}_0)$ and σ_1 by a closed curve Γ belongs to the resolvent set of $\mathcal{L}_0$ with $0 \in \Gamma$ and such that σ_0 belongs to the inner domain of Γ and σ_1 to the outer domain of Γ. Moreover, $\sigma_1 \subset [\theta_0, +\infty)$ with $\theta_0 = \inf\{\theta : \theta \in \sigma(\mathcal{L}_0), \ \theta > 0\} > 0$ (we recall that $\sigma_{\mathrm{ess}}(\mathcal{L}_0) = [1, +\infty)$). Then, by [51, Theorem 3.16, Chapter IV], we have $\Gamma \subset \rho(\mathcal{L}_Z)$ for $Z \in [-\delta_1, \delta_1]$ and $\delta_1 > 0$ small enough. Moreover, $\sigma(\mathcal{L}_Z)$ is likewise separated by Γ into two parts so that the part of $\sigma(\mathcal{L}_Z)$ inside Γ will consist of a negative eigenvalue with exactly total (algebraic) multiplicity equal to N. Therefore, by Proposition 3.8 we need to have $n(\mathcal{L}_Z) = N = 1$ for $Z \in [-\delta_1, \delta_1]$.

Next, using a classical continuation argument based on the Riesz-projection, we can see that $n(\mathcal{L}_Z) = 1$ for all $Z \in [0, +\infty)$ (see, e.g., the proof of Proposition 4.6 in [10]). This finishes the proof. □

The following result gives a precise value for the Morse-index of the operator $\mathcal{L}_Z$, with $Z \in (-\infty, -\frac{\pi}{2}c_1)$, when we consider the domain $\mathcal{C} \cap D(\mathcal{L}_Z)$, $\mathcal{C} = \{(u_j)_{j=1}^3 \in L^2(\mathcal{Y}) : u_1 = u_2 = u_3\}$. This strategy will allow the use of the linear instability framework established in Section 2 above. We call upon the attention of the reader that, in the present case, we do not know the exact value of the Morse-index of $\mathcal{L}_Z$ on the whole domain $D(\mathcal{L}_Z)$ (see Remark 3.12).

Proposition 3.11. *Let $c_1 = c_2 = c_3$ and $Z \in (-\infty, -\frac{\pi}{2}c_1]$. Consider $\mathcal{B} = \mathcal{C} \cap D(\mathcal{L}_Z)$. Then $\mathcal{L}_Z : \mathcal{B} \to \mathcal{C}$ is well defined. Moreover,* $\ker(\mathcal{L}_Z|_{\mathcal{B}}) = \{\mathbf{0}\}$ *and* $n(\mathcal{L}_Z|_{\mathcal{B}}) = 1$.

Proof. Initially, since $\varphi_1 - 2\pi = \varphi_2 = \varphi_3$ and $\cos(\varphi_1) = \cos(\varphi_1 - 2\pi) = \cos(\varphi_2) = \cos(\varphi_3)$ follows immediately that, for $\mathbf{u} = (u_j)_{j=1}^3 \in \mathcal{B}$, we have $\mathcal{L}_Z \mathbf{u} \in \mathcal{C}$.

Next, from the proof of Proposition 3.7 for $Z_0 = -\frac{\pi}{2}c_1$ we have $\ker(\mathcal{L}_{Z_0}|_{\mathcal{B}}) = \{\mathbf{0}\}$. Moreover, the anti-kink/kink profile for Z_0, $\Phi_0 = (\varphi_{1,0}, \varphi_{2,0}, \varphi_{2,0})$, satisfies that $\Phi_0' = (\varphi_{1,0}', \varphi_{2,0}', \varphi_{2,0}') \in \mathcal{C} \cap H^1(\mathcal{Y})$. Then, from (3.22) we know that the quadratic form Q_{Z_0} associated to $(\mathcal{L}_{Z_0}, \mathcal{B})$ satisfies $Q_{Z_0}(\Phi_0') < 0$. Therefore, $n(\mathcal{L}_{Z_0}|_{\mathcal{B}}) = 1$. Hence, by using a similar strategy as in the proof of Proposition 3.10 we obtain that $n(\mathcal{L}_Z|_{\mathcal{B}}) = 1$ for $Z \in (-\infty, -\frac{\pi}{2}c_1)$. This finishes the proof. □

Proof of Theorem 1.2. We consider initially the case $Z \in (-\frac{\pi}{2}c_1, +\infty)$. From Propositions 3.7, 3.8 and 3.10 we have $\ker(\mathcal{L}_Z) = \{\mathbf{0}\}$ and $n(\mathcal{L}_Z) = 1$. Moreover, from Section 3.2.2 and based in Proposition 3.3 we verify Assumption (S_1) for $J\mathcal{E}$ on $H^1(\mathcal{Y}) \times L^2(\mathcal{Y})$ in the linear instability criterion in Section 3.1. Thus, from Theorem 2.4 follows the linear instability property of the stationary anti-kink/kink soliton profile $\Pi_{Z,\delta'}$.

For the case $Z \in (-\infty, -\frac{\pi}{2}c_1]$ we need to adjust our instability criterion in Section 2 to the space $\mathcal{R} = (\mathcal{C} \cap H^1(\mathcal{Y})) \times \mathcal{C}$ determined by (3.14). Thus, initially we need to see that $J\mathcal{E}$ is the generator of a C_0-semigroup on the restricted subspace $\mathcal{R}$ (assumption (S_1)). Indeed, this is a consequence of the mapping $J\mathcal{E} : (\mathcal{C} \cap D(\mathcal{L}_Z)) \times (\mathcal{C} \cap H^1(\mathcal{Y})) \to (\mathcal{C} \cap H^1(\mathcal{Y})) \times \mathcal{C}$ is well defined and by using the same strategy as in Angulo and Plaza [11] (Section 3.1.1 and Proposition 3.11). Now, from Proposition 3.11 and Theorem 2.4 we finish the proof. □

Remark 3.12. In the general case where the constants c_j are not necessarily equal (see Propositions 3.8, 3.10 and 3.11), we do not know exactly the Morse index of $(\mathcal{L}_Z, D(\mathcal{L}_Z))$. From the analysis in Appendix B in [11], it is possible to have $n(\mathcal{L}_Z) \geqq 2$. We conjecture that these profiles are still unstable.

CRediT authorship contribution statement

Jaime Angulo Pava: Conceptualization, Methodology, Investigation, Writing – review & editing. **Ramón G. Plaza:** Investigation, Supervision, Writing – review & editing.

Declaration of competing interest

The authors declare that they have no known competing financial interests or personal relationships that could have appeared to influence the work reported in this paper.

Acknowledgments

J. Angulo Pava was supported in part by CNPq/Brazil Grant and by FAPERJ/Brazil program PRONEX-E - 26/010.001258/2016.

Appendix

For the sake of completeness, in this section we develop the extension theory of symmetric operators suitable for our needs. For further information on the subject the reader is referred to the monographs by Naimark [52,53]. The following classical result, known as *the von-Neumann decomposition theorem*, can be found in [54,55].

Theorem A.1. *Let A be a closed, symmetric operator, then*

$$D(A^*) = D(A) \oplus \mathcal{N}_{-i} \oplus \mathcal{N}_{+i}. \tag{A.1}$$

with $\mathcal{N}_{\pm i} = \ker(A^* \mp iI)$. Therefore, for $u \in D(A^*)$ and $u = x + y + z \in D(A) \oplus \mathcal{N}_{-i} \oplus \mathcal{N}_{+i}$,

$$A^* u = Ax + (-i)y + iz. \tag{A.2}$$

Remark A.2. The direct sum in (A.1) is not necessarily orthogonal.

The following propositions provide a strategy for estimating the Morse-index of the self-adjoint extensions (see Naimark [53]).

Proposition A.3. *Let A be a densely defined lower semi-bounded symmetric operator (that is, $A \geq mI$) with finite deficiency indices, $n_\pm(A) = k < \infty$, in the Hilbert space $\mathcal{H}$, and let $\widehat{A}$ be a self-adjoint extension of A. Then the spectrum of $\widehat{A}$ in $(-\infty, m)$ is discrete and consists of, at most, k eigenvalues counting multiplicities.*

Proposition A.4. *Let A be a densely defined, closed, symmetric operator in some Hilbert space H with deficiency indices equal $n_\pm(A) = 1$. All self-adjoint extensions A_θ of A may be parametrized by a real parameter $\theta \in [0, 2\pi)$ where*

$$D(A_\theta) = \{x + c\phi_+ + \zeta e^{i\theta}\phi_- : x \in D(A), \zeta \in \mathbb{C}\},$$

$$A_\theta(x + \zeta\phi_+ + \zeta e^{i\theta}\phi_-) = Ax + i\zeta\phi_+ - i\zeta e^{i\theta}\phi_-,$$

with $A^*\phi_\pm = \pm i\phi_\pm$, and $\|\phi_+\| = \|\phi_-\|$.

References

[1] G. Berkolaiko, An elementary introduction to quantum graphs, in: A. Girouard, D. Jakobson, M. Levitin, N. Nigam, I. Polterovich, F. Rochon (Eds.), Geometric and Computational Spectral Theory, in: Contemp. Math., Amer. Math. Soc., vol. 700, Providence, RI, 2017, pp. 41–72.
[2] R. Burioni, D. Cassi, M. Rasetti, P. Sodano, A. Vezzani, Bose–Einstein condensation on inhomogeneous complex networks, J. Phys. B: At. Mol. Opt. Phys. 34 (23) (2001) 4697–4710.
[3] J.-G. Caputo, D. Dutykh, Nonlinear waves in networks: Model reduction for the sine-Gordon equation, Phys. Rev. E 90 (2014) 022912.
[4] F. Fidaleo, Harmonic analysis on inhomogeneous amenable networks and the Bose–Einstein condensation, J. Stat. Phys. 160 (3) (2015) 715–759.
[5] D. Mugnolo (Ed.), Mathematical Technology of Networks, in: Springer Proceedings in Mathematics & Statistics, vol. 128, Springer, Cham, 2015.
[6] R. Adami, C. Cacciapuoti, D. Finco, D. Noja, Stable standing waves for a NLS on star graphs as local minimizers of the constrained energy, J. Differ. Equ. 260 (10) (2016) 7397–7415.
[7] Nonlinear dispersive equations on star graphs, in: 32o Colóquio Brasileiro de Matemática, IMPA, IMPA, 2019.
[8] J. Angulo Pava, N. Goloshchapova, Extension theory approach in the stability of the standing waves for the NLS equation with point interactions on a star graph, Adv. Differential Equations 23 (11–12) (2018) 793–846.
[9] On the orbital instability of excited states for the NLS equation with the δ-interaction on a star graph, Discrete Contin. Dyn. Syst. 38 (10) (2018) 5039–5066.
[10] J. Angulo Pava, R.G. Plaza, Instability of static solutions of the sine-Gordon equation on a $\mathcal{Y}$-junction graph with δ-interaction, J. Nonlinear Sci. 31 (3) (2021) 1–32, art. 50.
[11] J. Angulo Pava, R.G. Plaza, Unstable kink and anti-kink profile for the sine-Gordon equation on a $\mathcal{Y}$-junction graph with δ'-interaction at the vertex, 2021, Preprint arXiv:2101.02173v1.
[12] D. Mugnolo, D. Noja, C. Seifert, Airy-type evolution equations on star graphs, Anal. PDE 11 (7) (2018) 1625–1652.
[13] H. Susanto, S. van Gils, Existence and stability analysis of solitary waves in a tricrystal junction, Phys. Lett. A 338 (3) (2005) 239–246.
[14] H. Susanto, N. Karjanto, Zulkarnain, T. Nusantara, T. Widjanarko, Soliton and breather splitting on star graphs from tricrystal Josephson junctions, Symmetry 11 (2019) 271–280.
[15] A. Barone, F. Esposito, C.J. Magee, A.C. Scott, Theory and applications of the sine-Gordon equation, Riv. Nuovo Cimento 1 (2) (1971) 227–267.
[16] A. Barone, G. Paternó, Physics and Applications of the Josephson Effect, John Wiley & Sons, New York, NY, 1982.
[17] A.C. Scott, F.Y.F. Chu, S.A. Reible, Magnetic-flux propagation on a Josephson transmission line, J. Appl. Phys. 47 (7) (1976) 3272–3286.
[18] P.G. Drazin, Solitons, in: London Mathematical Society Lecture Note Series, vol. 85, Cambridge University Press, Cambridge, 1983.
[19] R. Knobel, An Introduction to the Mathematical Theory of Waves, in: Student Mathematical Library, American Mathematical Society, vol. 3, Providence, RI; Institute for Advanced Study (IAS, Princeton, NJ, 2000, IAS/Park City Mathematical Subseries.
[20] J. Frenkel, T. Kontorova, On the theory of plastic deformation and twinning, Acad. Sci. U.S.S.R. J. Phys. 1 (1939) 137–149.
[21] M. Cadoni, E. Franzin, F. Masella, M. Tuveri, A solution-generating method in Einstein-scalar gravity, Acta Appl. Math. 162 (2019) 33–45.
[22] E. Franzin, M. Cadoni, M. Tuveri, Sine-Gordon solitonic scalar stars and black holes, Phys. Rev. D 97 (12) (2018) 124018, 7.
[23] G. Derks, G. Gaeta, A minimal model of DNA dynamics in interaction with RNA-polymerase, Physica D 240 (22) (2011) 1805–1817.
[24] V.G. Ivancevic, T.T. Ivancevic, Sine-Gordon solitons kinks and breathers as physical models of nonlinear excitations in living cellular structures, J. Geom. Symmetry Phys. 31 (2013) 1–56.
[25] S.W. Englander, N.R. Kallenbach, A.J. Heeger, J.A. Krumhansl, S. Litwin, Nature of the open state in long polynucleotide double helices: possibility of soliton excitations, Proc. Natl. Acad. Sci. USA 77 (12) (1980) 7222–7226.
[26] L.A. Tahtadžjan, L.D. Faddeev, The Hamiltonian system connected with the equation $u_{\xi\eta} + \sin u = 0$, Tr. Mat. Inst. Steklova 142 (1976) 254–266, 271.
[27] M.J. Ablowitz, D.J. Kaup, A.C. Newell, H. Segur, Method for solving the sine-Gordon equation, Phys. Rev. Lett. 30 (1973) 1262–1264.
[28] M.J. Ablowitz, D.J. Kaup, A.C. Newell, H. Segur, The inverse scattering transform-Fourier analysis for nonlinear problems, Stud. Appl. Math. 53 (4) (1974) 249–315.
[29] A.C. Scott, F.Y.F. Chu, D.W. McLaughlin, The soliton: A new concept in applied science, Proc. IEEE 61 (10) (1973) 1443–1483.
[30] A.C. Scott, Nonlinear Science Emergence and Dynamics of Coherent Structures, second ed., in: Oxford Texts in Applied and Engineering Mathematics, vol. 8, Oxford University Press, Oxford, 2003.
[31] J.L. Bona, R.C. Cascaval, Nonlinear dispersive waves on trees, Can. Appl. Math. Q. 16 (1) (2008) 1–18.
[32] V.G. Kogan, J.R. Clem, J.R. Kirtley, Josephson vortices at tricrystal boundaries, Phys. Rev. B 61 (2000) 9122–9129.
[33] K. Sabirov, S. Rakhmanov, D. Matrasulov, H. Susanto, The stationary sine-Gordon equation on metric graphs: Exact analytical solutions for simple topologies, Phys. Lett. A 382 (16) (2018) 1092–1099.
[34] B.D. Josephson, Supercurrents through barriers, Adv. Phys. 14 (56) (1965) 419–451.
[35] C.C. Tsuei, J.R. Kirtley, C.C. Chi, L.S. Yu-Jahnes, A. Gupta, T. Shaw, J.Z. Sun, M.B. Ketchen, Pairing symmetry and flux quantization in a tricrystal superconducting ring of Y Ba_2 Cu_3 $O_{7-\delta}$, Phys. Rev. Lett. 73 (1994) 593–596.
[36] C.C. Tsuei, J.R. Kirtley, Phase-sensitive evidence for d-wave pairing symmetry in electron-doped cuprate superconductors, Phys. Rev. Lett. 85 (2000) 182–185.
[37] K. Nakajima, Y. Onodera, Y. Ogawa, Logic design of Josephson network, J. Appl. Phys. 47 (4) (1976) 1620–1627.
[38] K. Nakajima, Y. Onodera, Logic design of josephson network. II, J. Appl. Phys. 49 (5) (1978) 2958–2963.
[39] D. Dutykh, J.-G. Caputo, Wave dynamics on networks: method and application to the sine-Gordon equation, Appl. Numer. Math. 131 (2018) 54–71.
[40] A. Grunnet-Jepsen, F. Fahrendorf, S. Hattel, N. Grønbech-Jensen, M. Samuelsen, Fluxons in three long coupled josephson junctions, Phys. Lett. A 175 (2) (1993) 116–120.
[41] J. Angulo Pava, M. Cavalcante, Linear instability of stationary solutions for the Korteweg–de Vries equation on a star graph, Nonlinearity 34 (5) (2021) 3373–3410.
[42] A. Pazy, Semigroups of Linear Operators and Applications to Partial Differential Equations, in: Applied Mathematical Sciences, vol. 44, Springer-Verlag, New York, 1983.
[43] M. Grillakis, J. Shatah, W. Strauss, Stability theory of solitary waves in the presence of symmetry. II, J. Funct. Anal. 94 (2) (1990) 308–348.
[44] O. Lopes, A linearized instability result for solitary waves, Discrete Contin. Dyn. Syst. 8 (1) (2002) 115–119.
[45] J. Shatah, W. Strauss, Spectral condition for instability, in: J. Bona, K. Saxton, R. Saxton (Eds.), Nonlinear PDE's, Dynamics and Continuum Physics (South Hadley, MA, 1998), in: Contemp. Math., Amer. Math. Soc., vol. 255, Providence, RI, 2000, pp. 189–198.
[46] F.A. Berezin, M.A. Shubin, The Schrödinger Equation, Vol. 66, Kluwer Acad. Publ., Dordrecht, 1991.
[47] Methods of Modern Mathematical Physics. IV. Analysis of Operators, Academic Press – Harcourt Brace Jovanovich, Publishers, New York - London, 1978.
[48] J. Angulo Pava, O. Lopes, A. Neves, Instability of travelling waves for weakly coupled KdV systems, Nonlinear Anal. 69 (5–6) (2008) 1870–1887.
[49] J. Angulo Pava, F. Natali, On the instability of periodic waves for dispersive equations, Differential Integral Equations 29 (9–10) (2016) 837–874.
[50] D.B. Henry, J.F. Perez, W.F. Wreszinski, Stability theory for solitary-wave solutions of scalar field equations, Comm. Math. Phys. 85 (3) (1982) 351–361.
[51] T. Kato, Perturbation Theory for Linear Operators, Second ed., in: Classics in Mathematics, Springer-Verlag, Berlin, 1980.
[52] M.A. Naimark, Linear Differential Operators. Part I: Elementary Theory of Linear Differential Operators, Frederick Ungar Publishing Co., New York, 1967.
[53] Linear Differential Operators Part II: Linear Differential Operators in Hilbert Space, Frederick Ungar Publishing Co., New York, 1968.
[54] M. Reed, B. Simon, Methods of Modern Mathematical Physics. I. Functional Analysis, Academic Press, New York - London, 1972.
[55] Methods of Modern Mathematical Physics. II. Fourier Analysis, Self-Adjointness, Academic Press – Harcourt Brace Jovanovich, Publishers, New York - London, 1975.